

Review

# New Analytical Approaches for Effective Quantification and Identification of Nanoplastics in Environmental Samples

Christian Ebere Enyoh <sup>1,2,\*</sup> , Qingyue Wang <sup>1,\*</sup> , Tanzin Chowdhury <sup>1</sup>, Weiqian Wang <sup>1</sup> , Senlin Lu <sup>3</sup> , Kai Xiao <sup>1</sup>  and Md. Akhter Hossain Chowdhury <sup>4</sup>

- <sup>1</sup> Graduate School of Science and Engineering, Saitama University, 255 Shimo-Okubo, Sakura-ku, Saitama 338-8570, Japan; risha.chowdhury.bau@gmail.com (T.C.); weiqian@mail.saitama-u.ac.jp (W.W.); xiao.k.662@ms.saitama-u.ac.jp (K.X.)
- <sup>2</sup> Group Research in Analytical Chemistry, Environment and Climate Change (GRACE&CC), Department of Chemistry, Faculty of Physical Sciences, Imo State University, P.M.B 2000, Owerri 460108, Nigeria
- <sup>3</sup> School of Environmental and Chemical Engineering, Shanghai University, Shanghai 200444, China; senlinlv@staff.shu.edu.cn
- <sup>4</sup> Department of Agricultural Chemistry, Bangladesh Agricultural University, Mymensingh 2202, Bangladesh; akhterbau11@gmail.com
- \* Correspondence: cenyoh@gmail.com or enyoh.c.e.572@ms.saitama-u.ac.jp (C.E.E.); seiyo@mail.saitama-u.ac.jp (Q.W.)

**Abstract:** Nanoplastics (NPs) are a rapidly developing subject that is relevant in environmental and food research, as well as in human toxicity, among other fields. NPs have recently been recognized as one of the least studied types of marine litter, but potentially one of the most hazardous. Several studies are now being reported on NPs in the environment including surface water and coast, snow, soil and in personal care products. However, the extent of contamination remains largely unknown due to fundamental challenges associated with isolation and analysis, and therefore, a methodological gap exists. This article summarizes the progress in environmental NPs analysis and makes a critical assessment of whether methods from nanoparticles analysis could be adopted to bridge the methodological gap. This review discussed the sample preparation and preconcentration protocol for NPs analysis and also examines the most appropriate approaches available at the moment, ranging from physical to chemical. This study also discusses the difficulties associated with improving existing methods and developing new ones. Although microscopical techniques are one of the most often used ways for imaging and thus quantification, they have the drawback of producing partial findings as they can be easily mixed up as biomolecules. At the moment, the combination of chemical analysis (i.e., spectroscopy) and newly developed alternative methods overcomes this limitation. In general, multiple analytical methods used in combination are likely to be needed to correctly detect and fully quantify NPs in environmental samples.

**Keywords:** analytical techniques; characterization; sample treatment; fractionation; microscopy; light scattering; spectroscopy; mass spectrometry



**Citation:** Enyoh, C.E.; Wang, Q.; Chowdhury, T.; Wang, W.; Lu, S.; Xiao, K.; Chowdhury, M.A.H. New Analytical Approaches for Effective Quantification and Identification of Nanoplastics in Environmental Samples. *Processes* **2021**, *9*, 2086. <https://doi.org/10.3390/pr9112086>

Academic Editor: Guining Lu

Received: 21 October 2021

Accepted: 12 November 2021

Published: 22 November 2021

**Publisher's Note:** MDPI stays neutral with regard to jurisdictional claims in published maps and institutional affiliations.



**Copyright:** © 2021 by the authors. Licensee MDPI, Basel, Switzerland. This article is an open access article distributed under the terms and conditions of the Creative Commons Attribution (CC BY) license (<https://creativecommons.org/licenses/by/4.0/>).

## 1. Introduction

Approximately 80% of the 8 billion metric tons of plastic that has been manufactured to date has ended up in landfills or the environment [1,2]. Tiny pieces of plastic are formed through the fragmentation of bigger pieces, the use of synthetic fibers in clothes and the usage of microbeads in consumer goods [3]. These tiny pieces account for the majority of plastic particle counts in the environment and are typically referred to as microplastics (MPs, defined as particles with sizes greater than 100 nm and less than 5 mm). Nanoplastics (NPs  $\leq 100$  nm) particles, which are analogous to MPs particles, may also be created deliberately (primary NPs, which are manufactured for cleaning goods or as calibration standards for nanoparticles, for example) or from further degradation of MPs. By way of

illustration, ref. [4] reported the production of NP particles from millimeter-scale polymers using ultraviolet light. In the case of a PS disposable coffee cup lid, ref. [5] observed the production of NPs, while ref. [6] observed that MP particles (about 30  $\mu\text{m}$  in diameter) eaten by a planktonic crustacean (Antarctic krill) were broken into fragments smaller than 1  $\mu\text{m}$  in diameter. Due to their tiny size, NPs have the potential to be eaten by biota, with uncertain implications for the health of animals [7].

NPs are a rapidly developing subject that is relevant in environmental and food research, as well as in human toxicity, among other fields. The ability of nano-PET particles to penetrate the gut barrier was shown in a model of human intestinal epithelium, with uncertain long-term consequences on health as well as the possible transfer of related compounds as a result [8]. As a result of the high surface-to-volume ratio of NPs particles, it is anticipated that they would (ad)sorb greater quantities of external hazardous chemicals than MPs [9].

NPs have been recently recognized as one of the least studied types of marine litter, but potentially one of the most hazardous [8,10]. Thus, information on the chemical composition (including polymer type, additives and sorbed contaminants), number concentrations, size/size distribution and mass of NPs particles as well as on their shapes and surface properties are essential for the understanding of their impacts on the environment and human health.

In spite of several studies reporting on NPs in the environment including the North Atlantic surface water [11] and coast [2], Alpine snow [12] and soil [13] and in personal care products [14], the extent of contamination remains largely unknown due to practical and in some cases fundamental challenges associated with isolation and analysis. A knowledge gap exists as a result, particularly for polymers with a thickness of less than 100 nm. NP particles are diverse, in the same way as MP particles (e.g., polymer type, size, surface properties, etc.). However, structural diversity is expected to be lower than that of MP particles due to the significantly greater number of fragmentations that occur during the NPs formation process, as opposed to that of MP particles [15]. It is thus important for NP research to have knowledge and expertise from the MP domain. Due to the tiny mass and size of NPs, however, the techniques established for the analysis of MP particles can only be used to a limited extent to NP analysis.

It is the purpose of this research to investigate the analysis and separation of the lowest size fractions of plastics in the most difficult matrices. Techniques for NPs analysis are described in this paper in order to aid researchers in exploring new paths in the development of methods to isolate and analyze NPs in environmental samples. The analytical method framework for NPs analysis is presented in Figure 1. The different analytical steps are discussed in the following sections.

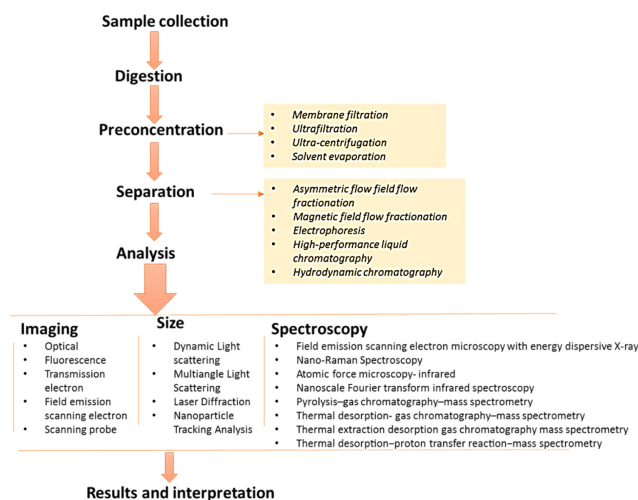


**Figure 1.** Analytical method framework for NPs analysis in environmental samples.

## 2. Sample Preparation or Preconcentration

Given the widespread presence of plastic contamination, the analytical procedure starts with defining the question to be answered (plastic particle quantity, size and PSD or mass of plastic particles per mass or volume of sample), which is dependent on the sample to be studied. Depending on the medium, sampling methods are varied and are akin to normal sampling processes for environmental samples. The sampling technologies for MPs are also applicable for NP, these techniques have been discussed previously [16,17]. The samples span from drinking water to food, as well as environmental fluids, sediments, biota tissue and in-/effluents from waste water treatment plants (WWTPs), all of which include different amounts of matrix around the plastic particles.

Prior to processing, samples are treated for undesirable organic materials (OM) by being digested with 30% hydrogen peroxide ( $H_2O_2$ ) for 7–8 days to remove the OM [7]. This percentage of hydrogen peroxide solution is suggested as an excellent reagent for the removal of about 50% of biogenic organic debris in one week [18]. In addition to these chemicals, perchloric acid ( $HClO_4$ ) and nitric acid ( $HNO_3$ ) can be used [5,18]. However, these chemicals must be properly prepared because aggressive chemicals such as these can be destructive to plastic particles if they are not properly diluted, resulting in inaccurate identification and quantification [19]. The amount of  $H_2O_2$  required for digestion is determined by the amount of organic matter (OM) present in the sample. It is important to note that the impact of the OM on the fate, effects and detectability of NPs is highly dependent on the particle size of the particles. In terms of the microscale, the OM is a tiny component when compared to the host polymer. As the size of the plastic component diminishes, the contribution of OM rises, and it becomes more difficult to distinguish the plastic component from the other components, particularly when the carbon-based structures are identical [8]. As a result, it is critical to eliminate OM from the samples prior to preconcentrating them.

NPs in the environment have very tiny sizes and masses and as a result, the pre-concentration step is almost always required throughout the analytical procedure [7]. Some of the pre-concentration methods that have been used are as follows:

### 2.1. Membrane Filtration

Membrane filtration is a widely used technique for removing particles from water samples due to its simplicity of use, high efficiency and desirable enrichment factors. Membranes with a range of pore diameters (from several  $\mu m$  to hundreds of nm) allow the fractionation of NPs of various sizes. Ref. [20] isolated NPs from teabag leachate after steeping plastic teabags at 95 °C using a cellulose filter. Polytetra-fluorethylene (PTFE) filters with a pore size of 0.2  $\mu m$  were also used to separate NPs from MPs in melting Alpine snow samples [12]. One of the primary advantages is that the size and shape of NPs retained on the filter may be maintained, allowing for subsequent identification and measurement. Membrane fouling, on the other hand, would significantly slow down the filtration process when the pore size is in the nm range [21,22] and the possibility of damaging pore structures would significantly reduce the amount of valid samples that can be filtered. Typically, the cost of membranes with smaller pore sizes of the same materials is much greater, which precludes the analysis of large volume samples. A progressive filtering process using membranes with varying pore sizes is a time-saving technique. Ref. [14] used a five-step filtering method using membranes of pore diameters of 20–25  $\mu m$ , 2.5  $\mu m$ , 0.45  $\mu m$  and two times 0.1  $\mu m$  for the size selection of PE NPs in face washes (Figure 2), which reduced pore clogging to a certain degree. Given that many membrane materials have a high capacity for adsorption of nanomaterials [23], the adsorption of NPs should also be considered. However, the filtering efficiency and recovery of NPs are seldom investigated, which may impair the subsequent analysis's accurate quantification of NPs.

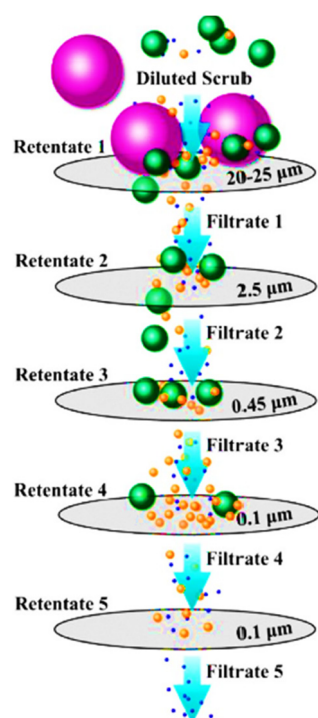


**Figure 2.** A flow diagram of the progressive filtering method used to remove PE NPs from commercial face scrubs. Ref [15] Reproduced with permission from Hernandez, et al., Environ. Sci. Technol. Lett., published by American Chemical Society, 2017.

Commercially available membrane filters with pore diameters ranging from several millimeters to 0.01 mm are made of various materials (e.g., aluminum oxide, ceramics, or polycarbonate). It should be mentioned that the use of polymeric membranes may result in contamination of the sample with plastic. Additionally, it should be remembered that the size fraction included in the filtrate is often lower than the nominal pore size. Membrane filters must be handled with extreme care to prevent harming the membrane and thus compromising the size cut-off.

## 2.2. Ultrafiltration

Ultrafiltration is a technique which enables the pre-concentration, separation and purification of NPs all in one step. Ultrafiltration utilizes nanoporous membranes with a molecular weight cut-off of between 5 and 50 nm. They are used in stirred cells [11], centrifugal fields [24], or cross-flow mode (also termed tangential flow) [25], in which the suspension flow is cycled through a parallel membrane to prevent it from being blocked. In this method, filtration is accomplished by applying pressure to the filtrate to aid in its flow, thus expediting the process.

A hydrostatic force is applied to a nanoporous membrane, allowing particles to be isolated from the solution [26]. Following ultrafiltration, a little amount of solvent is maintained, which facilitates particle collection and significantly minimizes sample loss, particle modification and aggregation. Researchers, such as [25,27,28], have used this technique to investigate NPs (1.2 μm or less) from artificially generated nanoparticles in aquatic environments. Ref. [11] concentrated 1 L of filtered seawater to 10 mL using an 8200-Amicon-stirred polysulfone 5 nm-based cell with a 100-fold enrichment factor while studying NPs in the North Atlantic subtropical gyre. Additionally, crossflow ultrafiltration is utilized to cleanse drinking water samples for the presence of NPs. Although repeatable, the recovery of 50 nm PS spheres was very low (12.7%), indicating that the method's effectiveness may be increased with further tuning [25].

### 2.3. Ultra-Centrifugation

Ultracentrifugation (UC) is a technique that takes use of high centrifugal force to investigate the characteristics of particles moving at very fast velocities. UC is enabled by a centrifuge, which is powered by an electric motor around a fixed axis. Using the sedimentation principle, a centrifuge operates by segregating substances according to their density when they are affected by gravitational force ( $g$ -force) [29]. The current generation of ultracentrifuges can spin at speeds of up to 150,000 rpm (equivalent to  $10^6 \times g$ ) [29]. For NPs, greater centrifugal forces in the region of  $10^5 \times g$  will be needed to impact the smaller plastic particles, which introduce the inherent problem of having densities near to that of water. Although this technology is widely accessible and easy to use, it only analyzes very small sample volumes, such as 10 to 100 mL, which limits its applicability to environmental water samples. Without separating the particles, ultracentrifugation collects all particles in the pellet, regardless of whether they are plastic or derived from the inorganic ambient matrix. Additionally, strong centrifugal pressures or the tension associated with redispersing the pellet may change the sample by forming aggregates or causing damage to the plastic particles [28,30]. On the other hand, these drawbacks may be irrelevant in an analytical procedure unaffected by sample morphology.

### 2.4. Solvent Evaporation

The solvent evaporation process from emulsion droplets is characterized by the removal of the polymer solvent from droplets containing the previously produced polymer (Figure 3). It is possible to create nanosized particles, despite the fact that the majority of studies deal with the production of microparticles [15]. This is typically accomplished by using ultrasonication to generate extremely tiny droplets, from which the solvent is evaporated [31] and an aqueous solution is used as the continuous phase. Several non-aqueous emulsions, including dimethylformamide-in-paraffin, dichloromethane-in-fluorinated solvent for microparticles and inverse systems in which water serves as the solvent have been described [32]. The technique is now extensively utilized to produce nanosized particles from a diverse range of polymers, including but not limited to semiconducting and biodegradable [33,34].

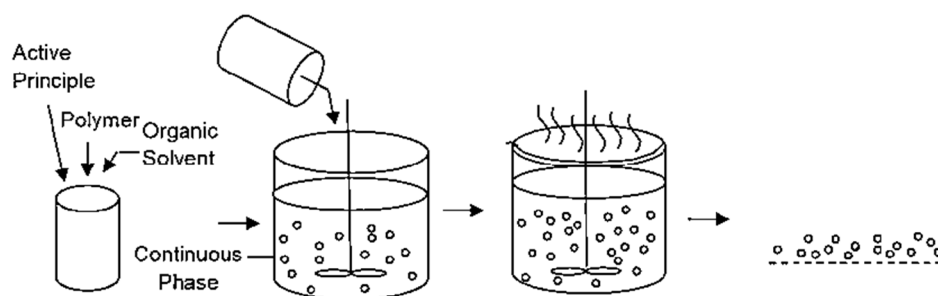


**Figure 3.** Solvent evaporation process. Ref [34] Reproduced with permission from Mehta et al. International Journal of Advanced Scientific Research; published by Gupta, 2016.

Solvent evaporation, which was initially utilized for nanoparticle production, is now being employed for NPs analysis. Mintenig [25] used this technique to analyze secondary PET NP suspensions (about 100 nm in size) in water, which were produced by laser ablation and then dissolved. They are widely accessible and easy to use, but some have disadvantages such as size specificity and the potential to capture other undesirable elements such as inorganic or organic material, among others. It is possible that this method will be most effective when used to concentrate suspensions from dialysis or cross-flow UF that are restricted in volume. This is due to the fact that this technology does not remove dissolved particles and is ineffective when removing huge quantities of water.

### 3. Sample Separation

Researchers have proposed methods for separating NPs in samples that were established for engineered nanoparticles and have proved to be useful for environmental NPs separation. These techniques are discussed in this section.

#### 3.1. Asymmetric Flow Field Flow Fractionation (AF4)

Asymmetrical flow field flow fractionation (AF4) is a well-established and state-of-the-art technique for fractionating and separating macromolecules and particles suspended in a liquid. In situations when column chromatography is not appropriate for the analyte, AF4 may be used in place of HPLC or SEC (discussed Sections 3.4 and 3.5). For liquid separations of molecules up to 1000 kDa and nanoparticles up to 10 nm, HPLC or SEC would be employed [15]. Once the size exceeds 10 nm, AF4 outperforms these techniques in terms of resolution and recovery [7].

The operating mechanism of the AF4 is shown schematically in Figure 4. In the focus stage (Figure 4a), two flows in opposing directions (fine blue arrows) are pushed into and balanced at the injection port by pumping them in from the inlet and exit ports. A narrow zone of focus is created by the two opposing flows of the focus stage, which concentrates the samples injected during the focus stage. The heights reached by particles are proportional to their diffusion coefficients. Particles with small hydrodynamic sizes and high diffusion coefficients elute at an early time point in the normal mode's elution stage (Figure 4b); on the other hand, particles with large hydrodynamic sizes and low diffusion coefficients elute later. However, when the physical size of a particle is too big ( $>1 \mu\text{m}$ ), when compared with the channel height, for it to be regarded a point mass, it elutes in the steric mode (Figure 4c) [35]. Here, particles are attracted to the membrane nearly equally strongly, but owing to their size, larger particles are subjected to greater laminar flow forces, leading them to elute more quickly than smaller ones. The mode point is determined by a variety of factors such as channel thickness, flow rate and cross-flow [36]. Due to the steric mode, this increases the possibility of co-elution of tiny and big particles, jeopardizing the separation. As a result, a separating step at the site of inversion, such as filtering, is recommended [25].

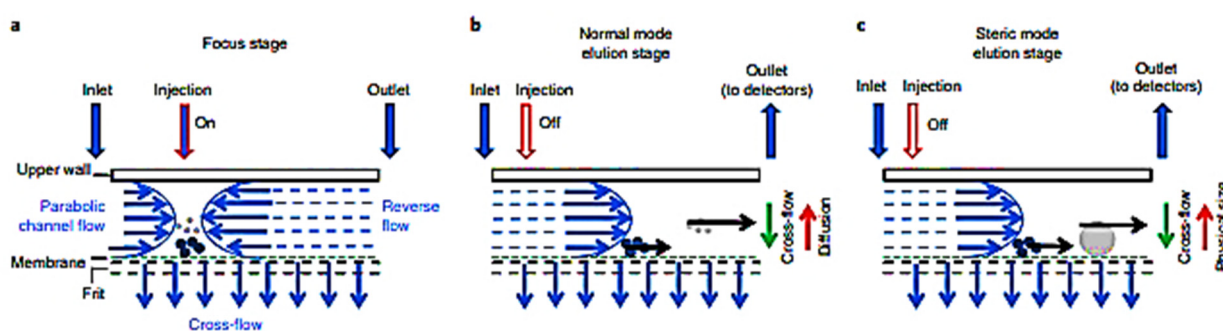


**Figure 4.** Diagrammatic representation of the AF4's operation. (a) In the elution step, the fine blue arrows represent the channel flow (horizontal arrows) and cross-flow (vertical arrows); the fine black arrows represent the channel flow that transports the nanoparticles through the channel (the lengths of the arrows represent magnitude of the flow rate); the thick blue arrows represent the inlet and outlet flows; and the red-outlined arrows represent the injection flow (the filled arrow indicates the injection flow is ON and the empty arrows indicate the injection flow is OFF). All of the arrowheads point in the direction of the flow. Fine green arrows indicate the direction of particle movement caused by cross-flow; fine red arrows in parts (b,c) denote the direction of particle movement due to their diffusion (b) or the physical position of particles in the channel as a result of their physical sizes (c). [35] Reproduced with permission from H. Zhang and D. Lyden, Nat. Protoc.; published by Nature 2019.

AF4 has been applied in the study of NPs. Gigault et al. [4] reported an AF4 technique designed for the rapid separation of primary NP PS beads with diameters ranging from 1 to 1000 nm. Loeschner and Correia [37] assessed a procedure for the characterization of primary NPs particles (PS 100 nm) in a fish tissue sample using Proteinase K to break-

down the matrix and AF4 based technique to separate the sample. AF4 can be used in tandem total organic carbon (TOC) (AF4-TOC) to enhance its efficiency, which was recently demonstrated by Mowla [38]. Using a combination of multimodal PS NPs in the presence of dissolved organic matter and clay colloids, they tested their approach. They came to the conclusion that the AF4-TOC approach provides a more robust and size-resolved quantification of NPs than other AF4 detection modalities, such as UV-Vis, refractive index and fluorescence tagging, which they compared. Mintenig [25] suggested the use of AF4 and Py-GC-MS (Section 4.3.5) for the study of plastic particles smaller than 20  $\mu\text{m}$  and verified the setup using primary PS particles ranging in size from 50 nm to 1000 nm suspended in drinking and surface water. In contrast, plastic particles in the environment are produced as a result of a variety of stressors that fracture the particle and typically oxidize the polymer [39], implying that the surface will be rough and negatively charged [5]. Techniques established for manufactured nanoparticles will need to be optimized for NPs particles owing to their densities, which will require adjusting the dispersion medium, flow rates and detector validation. Furthermore, validation must involve the identification of concentration ranges in order to conduct quantification.

### 3.2. Magnetic Field Flow Fractionation (MFFF)

Magnetic field-flow fractionation (MFFF) is a technique that utilizes variations in magnetic susceptibility to separate magnetic species [40]. In a nutshell, a magnetic force operates on a particle, compelling it toward the accumulation wall; this force is resisted by diffusion back into the flow stream, resulting in the formation of a steady-state particle distribution of a particular height. The hydrodynamic forces then operate perpendicular to the applied field, separating the components laterally.

MFFF exploits the magnetic characteristics of NPs as a result of their hydrophobicity, by magnetizing a sample of nanoparticles (e.g., iron, Fe, or platinum Pt) and then separating (magnetic extraction) and isolating them using magnetic fields [7]. NP particles are often drawn perpendicular to the direction of the flow [41]. Particles that interact weakly with the magnetic field have a high average layer thickness and elute more quickly; particles that interact strongly with the magnetic field have a lower average layer thickness and elute more slowly [7]. The method was applied in the study of [42]. They reported a recovery rate of 78% for polyethylene (PE), polystyrene (PS), polyurethane (PUR), polyvinyl chloride (PVC) and polypropylene (PP) from sediments. As a whole, the technique is very efficient for particles with sizes ranging from 20 nm to 1  $\mu\text{m}$  [7].

### 3.3. Electrophoresis

Electrophoresis is the movement of charged particles or atoms in an electric field. This happens when the substances are in aqueous solution as well as in solid phase [43]. The speed of movement is subject to the applied electric field strength and the charges of the atoms. Along these lines, differently charged atoms will form singular zones while they relocate [44]. Electrophoretic separation can occur through a gel (gel electrophoresis; GE) or through a column containing an electrolyte solution (i.e., capillary electrophoresis; CE). The separation method for NPs is based on the charges on their NP surfaces as they travel through an electric field-induced media (gel or electrolyte solution). The velocity of a particle is mostly determined by the intensity of the electrical field, the particle's net charge and the coefficient of friction (depended on size and mass of particle, compactness and porosity of the medium). Generally, for CE, it is essential to carefully regulate the surface charge using a surfactant [45]. These surfactants may, however, hinder further characterization of the NP particles [15].

### 3.4. High-Performance Liquid Chromatography (HPLC)

HPLC is a method for isolating, identifying and quantifying the constituents of a mixture. During the separation and analysis process, the sample mixture is introduced to the stream of mobile phase that is percolating down the column in a discrete little

quantity (typically microliters) [3]. Each of the sample components moves along the column at a different pace, which is controlled by their physical interactions with the adsorbent (also known as the stationary phase) (Figure 5). Each component's velocity is determined by its chemical composition, the stationary phase's nature (column) and the mobile phase's composition. The retention time of a particular analyte is the time at which it elutes (emerges from the column) [46]. Numerous column varieties are available, each with a unique combination of adsorbents with variable particle sizes, porosity and surface chemistry. Utilizing packing materials with smaller particle sizes demands a greater operating pressure ("backpressure"), which generally enhances chromatographic resolution (the degree of peak separation between consecutive analytes emerging from the column) [47].

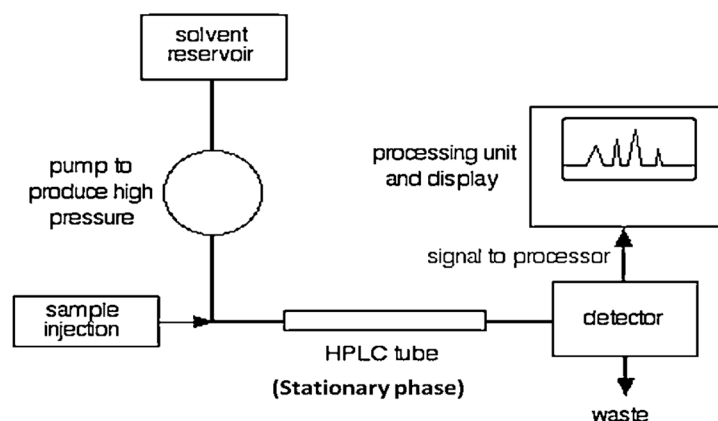


Figure 5. HPLC process scheme.

Regular HPLC column and its narrow pore size made it difficult in determining nanoparticles of 40 nm diameter. However, with special columns, this can be easily achieved. Currently, HPLC are extensively utilized to characterize manufactured nanoparticles with sizes ranging from 1 nm to 40 nm [48,49]. As a result, they may also be relevant to the separation of NPs. In comparison to nanoparticles, NPs particles formed during fragmentation are anticipated to have rougher surfaces, potentially increasing their contact with the stationary phase. Another factor to consider is the density differential between manufactured nanoparticles and natural nanoparticles, which requires the maintenance of a stable suspension [50].

### 3.5. Size Exclusion Chromatography (SEC)

SEC is a type of HPLC that is mainly utilized for the study of big molecules, such as polymers, rather than for smaller molecules. Adsorbents function by trapping smaller molecules in their pores ("stationary phase"). SEC procedure is carried out inside a column, which is generally comprised of a hollow tube densely packed with nano-scale polymer beads with holes of varying diameters. These pores may be depressions on the surface of the bead or channels running through it. As the solution moves down the column, particles are drawn into the pores by diffusion. Larger particles are unable to penetrate as many pores as smaller ones. The elution rate increases with the size of the particles [7]. The bigger molecules just pass through the pores because they are too massive to fit through the pores in the first place. As a result, larger molecules pass down the column more rapidly than smaller ones, resulting in a retention period that is greater the smaller the molecule. The SEC is effective for NPs within the range of 1 nm to 100 nm [51].

In real-world circumstances, particles in solution do not have a fixed size, which increases the likelihood that a particle that would be harmed by a pore would pass directly past it. Additionally, the particles in the stationary phase are not well defined; both particles and pores may vary in size. The stationary phase may interact negatively with a particle and affect retention durations, but column manufacturers take great effort to

select innocuous stationary phases that minimize this problem [52]. As with other types of chromatography, extending the length of the column improves resolution, while increasing the diameter of the column increases column capacity. Proper column packing is critical for achieving the highest possible resolution: It is possible that a column that is too tightly packed may force the pores in the beads to rupture, resulting in a loss of resolution. The percentage surface area of the stationary phase that is accessible to smaller species may be reduced in a column that is not packed firmly enough, resulting in those species spending less time trapped in pores. When compared to affinity chromatography, the presence of a solvent head at the top of the column may substantially impair resolution by increasing the width of the downstream elution zone [7].

### 3.6. Hydrodynamic Chromatography (HDC)

Hydrodynamic chromatography is like SEC, with the exception of the non-permeable nature of the stationary phase; there are less conceivable outcomes of solid phase associations. This method is effective for particle between 5 nm to 1200 nm. A robust size characterization methodology for studying nanoparticle behavior in 'real' environmental samples, using hydrodynamic chromatography coupled to ICP-MS [53].

## 4. Quantification and Identification Techniques

The final analytical process before the reporting of results includes the use of different spectroscopic or spectrometric techniques for imaging, size determination, identification and quantification.

### 4.1. Imaging (Microscopy) Techniques

Microscopy methods have existed for decades and are constantly being improved. The discipline has had to develop as the samples examined have become smaller and smaller, particularly since nanomaterials have made their way into a variety of fields of research. Each microscopy method has benefits and drawbacks that make it better suited to certain samples and research situations and in this section, the appropriateness of microscopy for studying NPs is discussed.

#### 4.1.1. Optical Microscopy

The optical microscope, often known as a light microscope, is a kind of microscope that typically use visible light and a lens system to magnify tiny objects. Optical microscopes are the most primitive kind of microscope, probably developed in its current compound form in the 17th century. Although many sophisticated designs seek to increase resolution and sample contrast, basic optical microscopes may be very simple. The item is staged and seen directly via one or two of the microscope's eyepieces.

Optical microscopes are excellent for examining items visible to the human eye in greater detail, as well as micron-sized materials. They do, however, lack the capacity to examine nanostructured materials in great detail, since their greatest magnification is only 1000x and their highest resolution is just 200 nm [54]. This is larger than the size of the majority of nanomaterials and, although they may sometimes be seen with an optical microscope, the various properties of the nanomaterial are not visible. There are several adaptations being explored to reduce the resolution to the nanoscale region, one of which is the inclusion of plasmonic gratings and using a smallest condenser aperture (i.e., using low partial coherence) [55]. With early prototypes developed in an academic laboratory achieving a resolution as low as 3 nm [55], optical microscopes may soon become a viable method for nanoscale microscopy.

Studies on the quantification of NPs using optical microscopy are still in their infancy. Chae [56] showed the use of optical microscopy with a fluorescence filter to investigate PS-NPs in a four-species freshwater food chain using a fluorescent filter. The effects of fluorescent PS NPs (100 nm) on trophic transfer, individual impact and embryonic uptake in a freshwater environment were studied in this research via direct contact to the particles

with four species, namely the alga (*Chlamydomonas reinhardtii*), water fea (*Daphnia magna*), secondary-consumer fish (*Oryzias sinensis*) and end-consumer fish (*Zacco temminckii*). Another study by [57] utilized optical microscope to study PS NPs toxicity on green microalgae *Chlorella vulgaris*. The findings of the research demonstrated that optical microscopy may be used to track the transit of NPs ingested by organisms.

#### 4.1.2. Fluorescence Microscopy

Unlike an optical microscope, which depends on the contrast of the picture created by light reflecting off the sample, a fluorescence microscope gathers fluorescent emission from materials stimulated at a particular wavelength. When the laser light strikes and excites this material, it produces fluorescence light. Traditionally, the laser beams continuously in the visible (blue) and ultraviolet (UV) ranges pass through a small hole (pinhole) and focus on a specific spot on the sample to be examined. Due to the short wavelength, each fluorophore molecule that is activated by a photon produces fluorescence in the focus and the surrounding region. As the incoming photon must provide more energy, the exciter laser's wavelength must be 50–200 nm shorter than the light produced by the fluorophore [58].

In the analysis for NPs using this technique, the NPs sample are either exposed to a chemical that acts as fluorophore, e.g., Nile Red, to mark plastic particles, particularly when tissues or organisms are analyzed [9,59], or target directly based on their intrinsic capacity to emit fluorescence, especially for white and clear plastics Micro and Nanoplastics Identification: Classic Methods and Innovative Detection Techniques [60].

Fluorescence microscopic technique has been used in the study of NPs (Figure 6) [61], which applied the method to study polystyrene (PS) NPs of size 50 nm intake by the *T. japonicas* copepod (Figure 6A). Another study conducted by [62] on an edible plant lettuce using fluorescent markers investigated the uptake, distribution and migration of two sizes of PS microbeads (200 and 1000 nm) in the plant (Figure 6B). These studies showed the efficiency of using fluorescence microscopy mainly for particles within tissues. However, the investigation of NPs' evidence for biological membrane crossing has been inconclusive thus far, as labeled NPs solutions may contain residual free dye that peels off in an altered medium properties (i.e., pH, electrical conductivity, or salinity, etc.) and the intensity of total fluorescence in cells following exposure can be mistakenly attributed to the presence of nanoparticles when it is actually caused by free fluorophore [63]. Another constraint on the visibility of NPs is the chemical additives employed in the manufacturing process, which may affect the fluorescence characteristics as well. For instance, additives may possess luminous characteristics and therefore obstruct microscopic fluorescence measurements [64]. As a result, sufficient pretreatment is required to remove as many of these contaminants as feasible. Typically, acids or oxidants (e.g., hydrogen peroxide) are employed to clean the surface, followed by enzymatic digestion [7,9]. These pretreatments remove surface impurities or pollutants, but do not eliminate the possibility of inferences from the chemicals contained in NPs [60].

#### 4.1.3. Transmission Electron Microscopy (TEM)

The electron microscope has an extremely high resolution that enables viewing of materials with microscopic sizes due to the wave characteristics of electrons produced by a very thin filament of thermoionic material or by a field emitter source for top-level TEMs. The electrons are then introduced into the magnetic capacitor through a hole in the anode (the capacitor has the purpose of regulating the intensity of the convergence of the electron beam). Transmission electron microscopy (TEM) is the most often used method for characterizing nanomaterials in electron microscopy, giving chemical information and pictures of nanomaterials with a spatial resolution comparable to that of atomic dimensions [65].

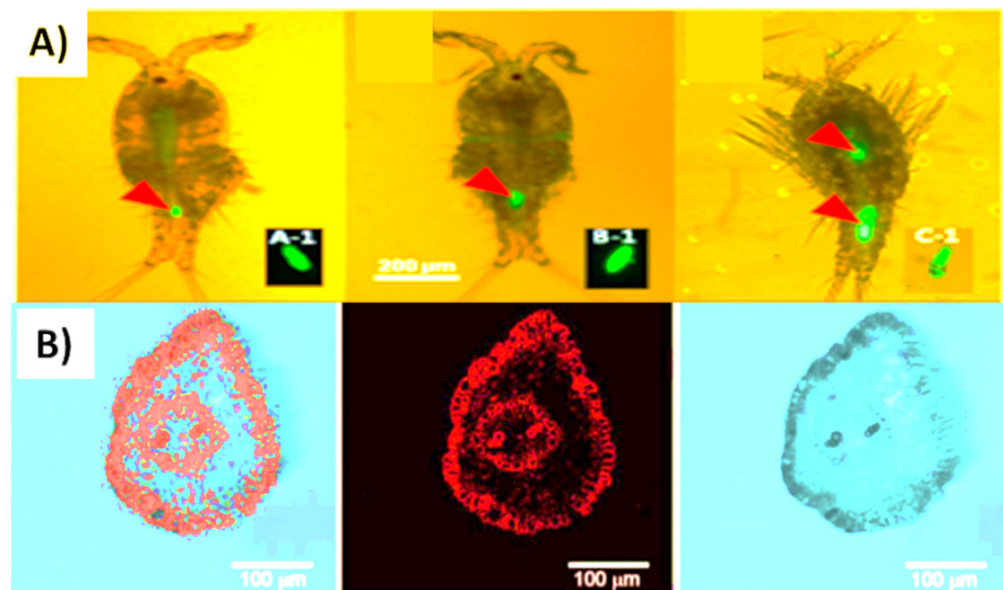


**Figure 6.** Fluorescently tagged PS beads of (A) 50 nm intake by *T. japonicas* copepod Reproduced with permission from Lee et al. Environmental Science & Technology; published by American Chemical Society, 2013. (B) 200 nm uptake by lettuce root and stem. Ref [61,62] Reproduced with permission from Li et al., Chinese Sci. Bull.; published by Elsevier 2019.

In nanoparticle research, conventional TEM is widely used to describe particle structure [66], to show the intracellular location of nanoparticles [67,68] and to define particle morphology [69]. This method is now being extended to NP research. For example, [70] investigated the toxic effects of polystyrene NPs on the marine bacterium *Halomonas alkaliphila* by using TEM. They were able to detect an increase in extracellular polymeric compounds as potential bacterial defensive strategies. In another research, TEM characterization was used to assess the potential impact of small plastics particles (PP, PE, PET and PVC) on microalgae, including growth suppression and cell structural modification [71]. Wang [72] monitored the exposure of marine microalgae *Platymonas helgolandica* exposed to 70 nm PS NPs for 96 h using TEM, while [73], using the same PS NPs (20, 50 and 500 nm), evaluated its toxicity to microalgae (*Chlorella vulgaris*).

Particles that are seen in TEM images, on the other hand, are often agglomerated formations with diameters that are much more than 100 nm. As a result, excessively low magnifications are used, which prevent the identification of particles in the range of 10–20 nm or even smaller from being possible. Furthermore, it is often overlooked that NPs may occasionally be indistinguishable from cellular structures that are in the same size range as the NPs. Electron lucent particles (for example, PS) may be confused with spherical microvesicular structures, requiring visualization and quantitative analysis of nanoparticles in the respiratory tract by transmission electron microscopy [74]. Therefore, there is the possibility of technical bias being present, either as a result of cellular structures being confused for NP or vice versa, and this is something to be cautious about. This bias cannot be addressed by using just standard TEM techniques. For example, in Figure 7, in A, five polystyrene NPs with a mean diameter of 78 nm are seen adjacent to an A549 cell, also with a diameter of 78 nm. Once they have been taken up by the cells, they may take on the look shown in B. It is very probable that the spherical structures in B (NP?) are not NPs, but vesicular structures such as caveolae.

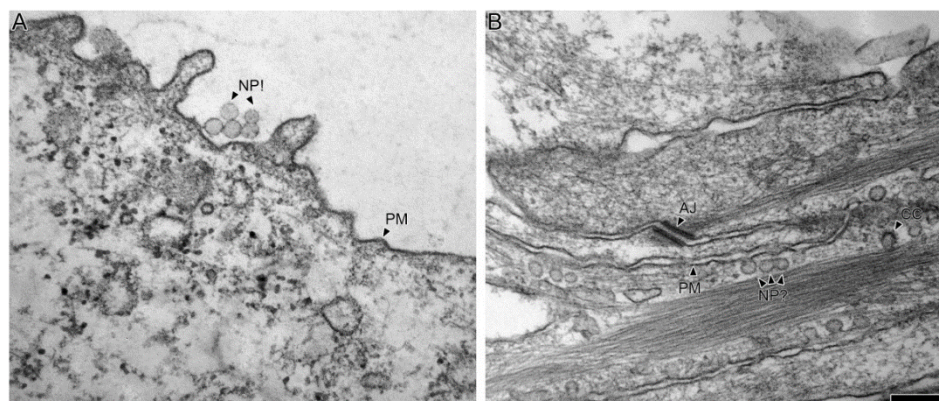


**Figure 7.** PS NPs imaged with a conventional transmission electron microscope. This image shows the difficulty of distinguishing clearly between NPs (A) and cellular structures (B) using standard transmission electron microscopy. CC stands for clathrin coated vesicle; PM is for plasma membrane; and AJ stands for adherens junction. Ref [74] Reproduced with permission from Mühlfeld et al., Particle and Fibre Toxicology; published by BioMed Central, 2007.

Another disadvantage of TEM is the lengthy and complex sample preparation needed, which includes fixation, dehydration, drying, embedding, trimming and cutting, and heavy metal staining [75]. Centrifugation and cell fixation procedures have the potential to change membrane characteristics, resulting in erroneous nanoparticle uptake [76]. Despite its widespread usage in NPs research, conventional TEM should not be used as a single tool for the qualitative or quantitative assessment of the cellular localization of NPs without first doing a thorough case-by-case review. Therefore, it must be supplemented with techniques that improve the identification of each NP regardless of its size, shape, or electron transmissibility. Conventional TEM, on the other hand, is acceptable in its use because of its capacity to identify possible impacts of nanoparticles on cellular ultrastructure as well as to describe the structure of NPs.

#### 4.1.4. Field Emission Scanning Electron Microscopy (FE-SEM)

Field emission scanning electron microscopy (FE-SEM) is a microscopic technique that may be used to get information on the morphological surface structure of nanoparticles in samples by generating high-resolution images in the range of 10–300,000 $\times$  [77] of the surface state. Due to its greater resolution, FE-SEM is often employed when SEM characterization of a given sample does not provide a clear or acceptable morphology. The spatial resolution of the FE-SEM is <1 nm and it offers a number of additional benefits, including much better performance at low accelerating voltages [75]. These characteristics of FE-SEM have enabled the development of novel methods for studying NPs, based on high resolution images previously only available through TEM. For example, ref. [78] used the FE-SEM to study small MPs (100 nm) in sediment samples collected in the Northern coast of the Persian Gulf, while ref. [57] utilized it to study PS NPs toxicity on green microalgae *Chlorella vulgaris*. These studies showed that the method enables the acquisition of high-quality and high-magnification pictures without the need for additional sample preparation prior to observation. Furthermore, it is a simple and rapid method since no metal or carbon is required to cover the sample; instead, small particle pieces are immediately put on the carbon tape on the aluminum stub. However, in general, FE-SEM may be used to quantify NPs in the range of 15 nm to 100 nm [79].

#### 4.1.5. Scanning Probe Microscopy (SPM)

Scanning probe microscopy (SPM) is a kind of microscopy in which pictures of surfaces are created by scanning the specimen with a physical probe. Scanning Probe Microscopy (SPM) techniques such as Scanning Tunnelling Microscopy (STM), Scanning Force Microscopy (SFM), Magnetic force microscopy (MFM) and Atomic Force Microscopy

(AFM) have demonstrated exceptional performance in resolving structures with sub-nanometer details, the shape of a nanostructure, its surface topography and its local electric properties [8,60].

Numerous scanning probe microscopes are capable of concurrently imaging several interactions. The way in which these interactions are used to generate a picture is referred to as a mode. Table 1 summarizes the most frequently used SPM imaging modalities for nanoparticle characterization. Although resolution varies somewhat across methods, certain probing techniques achieve an amazing atomic resolution. This is mainly because piezoelectric actuators can perform movements with atomic precision or better when controlled electronically. This method family is referred to as piezoelectric techniques [80]. The second common denominator is that the data is usually acquired in the form of a two-dimensional grid of data points, which is then displayed in false color as a computer picture.

**Table 1.** Most common SPM imaging modes applied for characterizing nanoparticles.

SPM Mode	Probe Type	Parameters Measured
Contact mode and frictional force AFM	Silicon, silicon nitride	Surface profiles, morphology, height changes, frictional forces
Tapping mode AFM and phase imaging	Silicon, silicon nitride	Surface profiles, morphology, height changes, elastic response
STM	Metal wire	Surface profiles, morphology, changes in sample currents
MFM	AFM probe with a magnetic coating	Surface profiles, morphology, relatively long-range magnetic forces
Magnetic sample modulation (MSM) AFM	Silicon, silicon nitride	Surface profiles, morphology, magnetic response induced for individual nanoparticles, changes in vibration amplitude and frequency

The resolution of the microscopes is not restricted by diffraction, but rather by the volume of the probe-sample interaction (i.e., the point spread function), which may be as tiny as a few picometres. As a result, the capacity to detect tiny local variations in object height (such as 135 picometre steps) is unmatched. Laterally, the probe-sample contact is limited to the interaction's tip atom or atoms. The interaction may be utilized to manipulate the sample in order to generate microstructures (Scanning probe lithography). Unlike electron microscopy, scanning probe lithography does not need a partial vacuum; instead, specimens may be viewed in ambient air or immersed in a liquid reaction tank [81].

Despite their many benefits, SPM methods as stand-alone tools have certain limitations: Not only are they incapable of performing atomic or molecular identification, but they also usually provide little or no chemical information. It is sometimes difficult to identify the precise geometry of the scanning tip. Its impact on the resultant data is most apparent when the specimen's height changes significantly across lateral distances of less than 10 nm. Due to the scanning process, scanning methods are typically slower in acquiring pictures. As a consequence, significant efforts are being undertaken to increase the scanning rate for chemical analysis at the nanoscale [82,83], indicating that these techniques have a great deal of promise in the area of nanoparticle research. AFM is one of the nanoscale methods available. The benefit of utilizing AFM over other microscopy techniques such as scanning tunneling or electron microscopy is that samples do not have to be conductive; both conducting and insulating nanomaterials may be examined without modification. Furthermore, AFM may be used to produce excellent views of samples in both air and liquid media without the need for a vacuum chamber, which is another benefit. While the contact mode and tapping mode are the most often used imaging modes for AFM, there are a variety of additional modes that need particular changes to the instrument setup [80].

AFM has been widely utilized to characterize a variety of nanoscale materials, ranging from manufactured nanoparticles to soil particles, polymeric membranes and other nanostructures [60]. Thus, AFM is a potential approach for characterizing NPs, but it must be used in conjunction with other methods.

## 4.2. Size Determination Techniques

### 4.2.1. Dynamic Light Scattering (DLS)

Dynamic light scattering (DLS) is a method for determining the size distribution profile of tiny particles or polymers suspended in solution. Temporal fluctuations are often studied using the intensity or photon autocorrelation function in the context of DLS (also known as photon correlation spectroscopy or quasi-elastic light scattering).

The framework of the DLS method is presented in Figure 8. If a nanoparticle suspension is exposed to a light beam (electromagnetic wave) during the DLS measurement, a process called scattering occurs, which causes the direction and intensity of incoming light to alter when the particle impinges on the light beam [85]. Due to the fact that the nanoparticle is in continuous random motion as a result of their kinetic energy, the change in intensity with time includes information about that random motion and may be utilized to determine the particles' diffusion coefficient [86]. For spherical particles, the hydrodynamic radius of the particle  $R_H$  may be determined using the Stokes–Einstein equation, i.e.,

$$D_f = k_B T / 6\pi\eta R_H \dots \dots \quad (1)$$

where  $k_B$  = Boltzmann constant,  $T$  = suspension's temperature,  $\eta$  = surrounding media's viscosity. The hydrodynamic radius is the diameter of a sphere with the same diffusion coefficient as the particles being measured when it is placed in the same viscous environment [84,87].

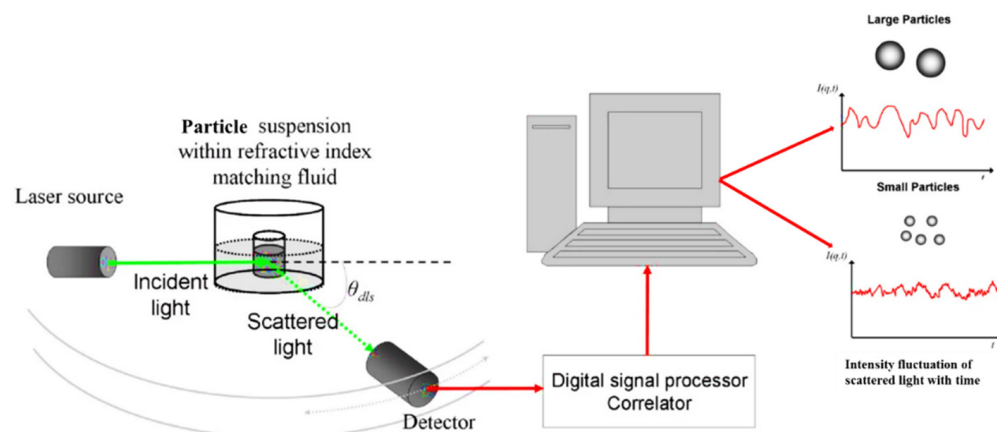


**Figure 8.** Optical arrangement of a common experimental setup for studies of dynamic light scattering. Ref [84] Reproduced with permission from Lim et al., *Nanoscale Research Letters*; published by Springeropen, 2013.

DLS offers a number of benefits for sizing nanoparticles and has been extensively utilized to estimate the hydrodynamic size of a variety of NPs. Ref. [88] was able to determine the size of PMMA NPs in solution to be 59–85 nm using the DLS method. DLS measurement takes just a few seconds and is nearly entirely automated, which means the whole process is less labor intensive and does not need significant expertise. Additionally, this method is non-invasive, and the sample may be reused after the assessment, a property that is critical for recycling NPs. Since the strength of scattering is exactly related to the sixth power of the particle radius, this method is very sensitive to the existence of tiny aggregates [87]. As a result, even with the occurrence of restricted aggregation events, erroneous measurement may be successfully avoided.

### 4.2.2. Multiangle Light Scattering (MALS)

Multiangle light scattering (MALS) is a method for determining the angle of light dispersed by a particle. By observing how particle scatter light, it is possible to determine both the absolute molar mass and the average size of the particle in solution. The method is most often employed with collimated light from a laser source, in which case it is

referred to as multiangle laser light scattering (MALLS) [89]. MALS is frequently used in conjunction with size fractionation techniques such as SEC or field-flow fractionation (FFF), which enables direct determination of the average molar mass and root mean-square radius of each eluted fraction without calibration against standards or making assumptions about polymer shape [90]. This method was recently used in studying the size of nanoparticles [91], therefore suggests that it can be used in the study of NPs.

#### 4.2.3. Laser Diffraction (LD)

In laser diffraction analysis (LDA), also known as laser diffraction spectroscopy, the diffraction patterns of a laser beam passed through any object with diameters ranging from nanometers to millimeters are measured in order to determine the geometrical dimensions of a particle in a relatively short period of time. Neither the volumetric flow rate nor the amount of particles flowing through a surface over time have any effect on this process [92].

A preferable technique for determining particle size and distribution across a broader range of particle sizes (20 nm–2000 nm) is the use of laser desorption (LD) [93]. For particle size measurement, it may be used in conjunction with the DLS. Using the Mie theory, it is possible to compute the equivalent sphere diameter of particles. In order to determine particle size, it is necessary to take into consideration the fact that smaller particles scatter the laser beam at wide angles, whereas bigger particles scatter light at smaller angles. Particle sizes of less than one micron are measured using blue lasers, whereas particle sizes of more than one micron are measured with red lasers [94].

#### 4.2.4. Nanoparticle Tracking Analysis (NTA)

Nanoparticle Tracking Analysis (NTA) is a technique for viewing and studying particles in liquids that correlates the rate of Brownian motion with particle size. The velocity of the liquid is determined only by its viscosity and temperature; it is unaffected by particle density or refractive index. NTA is presently capable of processing particles with a diameter of about 10 to 1000 nm, depending on the kind of particle [44]. Only particles comprised of materials with a high refractive index, may be analyzed at the low end of this spectrum.

The method is combined with an ultramicroscope and a laser illumination device to view tiny particles in liquid suspension moving in Brownian motion. A charge-coupled device (CCD) camera captures the light dispersed by the particles across a series of frames. The motion of each particle between frames is then tracked using computer software. The rate of particle motion is proportional to the Stokes–Einstein equivalent hydrodynamic radius of a sphere (see Equation (1)) [95] just as in DLS. Unlike DLS, which is based on a digital correlator, NTA is based on video clips, allowing for precise characterization of real-time processes such as aggregation and dissolution [96]. Sizing and phenotyping of cellular vesicles using nanoparticle tracking analysis. Overall, sample preparation is minimal, which reduces the amount of time needed to process each sample.

### 4.3. Chemical Identification and Characterization

#### 4.3.1. Field Emission Scanning Electron Microscopy with Energy Dispersive X-ray (FESEM-EDX)

If combined with energy dispersive X-ray (EDX) microanalysis and backscattered electron imaging (BEI), FE-SEM may serve as an excellent analytical method for defining and visualizing the elemental composition of the NPs particle, as shown in Figure 9. EDX is a technique that relies on the interaction of an X-ray source and a specimen. Its capacity to characterize elements is due in large part to the fundamental idea that each element has a unique atomic structure, which results in a distinct collection of peaks on its electromagnetic emission spectrum when seen from different angles [97,98]. FE-SEM coupled with EDX was used in the study of [78] and a typical result is presented in Figure 9.

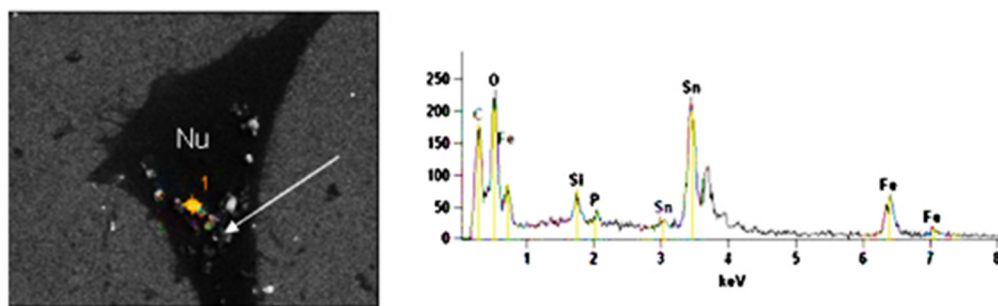


**Figure 9.** Typical FE-SEM/EDX result. Ref [78] Reproduced with permission from Naji et al., Mar. Pollut. Bull.; published by Elsevier, 2019.

#### 4.3.2. Nano-Raman Spectroscopy

The scattering of light at a molecule includes information about the molecular vibration and this scattering phenomenon is referred to as Raman scattering. Raman scattering spectroscopy has been extensively utilized to analyze molecules and crystal lattices.

Tip-enhanced Raman spectroscopy (TERS) is a technique that combines Raman spectroscopy with a fine metallic tip that may be used to probe extremely near to the sample surfaces. Nanoscale spatial resolutions are possible because of the extremely confined and substantially increased optical field produced by the tip apex in close proximity to the tip [99]. The term “nano-Raman Spectroscopy” refers to Raman spectroscopy with nanoscale resolution.

TERS employs an AFM or STM to scan a plasmonic metal nanostructure over a sample surface in order to increase the electromagnetic field locally [100]. The enhanced electromagnetic field is the result of a combination of two distinct physical effects: the “lightning rod” effect, which is caused by the geometric singularity associated with sharply pointed metal structures, and the LSPs (Localized Surface Plasmons), which are strongly dependent on the excitation wavelength and are geometry-dependent. The laser excitation light is directed onto the very tip of the sharp metal tip, which is maintained in close proximity to the nanoparticle surface. LSPs are stimulated at the apex of the tip or in the cavity between the tip and the material, and only the molecules directly under the tip in the increased field exhibit strong Raman scattering. The tip functions as an amplifier for incoming and outgoing electromagnetic waves, allowing for very strong Raman scattering [99].

TERS has been utilized in a variety of applications, including material characterization, cell identification and device characterization. Zhu [101] showed that by detecting a double band, strained Si lines with a width of 10 nm may be resolved. Ref. [102] imaged individual nanoparticles using nano-Raman spectroscopy. Nowadays, TERS systems are available in a variety of configurations, including bottom-, top- and side-illumination, as well as parabolic mirror-based setups that enable sensitive chemical analysis with spatial resolutions of approximately 30 to 50 nm and in some cases as low as 1.7 nm [8]. TERS has the potential to provide nanoscale resolved chemical information on NPs particles, but as of now, only one study has reported on the TERS analysis of a 20 nm NPs made of PS and polyisoprene, PI blends [103]. This study suggested that the applicability of this very promising technique in the field of NPs, which remains unexplored.

Using optical tweezers, NPs was studied directly in aqueous media. The optical tweezers keep the particles in the focus of the laser beam, allowing for spectroscopic identification to be accomplished. For the trapping and chemical identification of nanoparticles, [104] recently demonstrated the applicability of a method combining optical tweezers with Raman spectroscopy by investigating the behavior of plastic particles (PE, PP and PS), polyester fibers (PET), polyvinyl chloride (PVC), polymethyl methacrylate (PMMA) and polyamide 6 (PA 6) distributed in seawater using excitation lasers at 633 and 785 nm. The authors were able to distinguish clearly between plastics and organic materials as well as mineral sediments, as well as determine the size and form of NMPs (beads, pieces and fibers), with spatial resolution only limited by diffraction, as a result of their single particle

analysis. It was shown that the technique works on both model particles and naturally aged environmental samples, indicating that it has promise for use in the characterization of actual samples [104].

#### 4.3.3. Atomic Force Microscopy-Infrared (AFM-IR)

AFM-IR (atomic force microscope-infrared spectroscopy, or infrared nanospectroscopy) is one of a series of methods that evolved from the merging of two parent instrumental techniques. AFM-IR blends infrared spectroscopy's chemical analysis capability with the high spatial resolution of SPM [105]. The name was originally used to refer to a technique that coupled a tunable free electron laser with an atomic force microscope (AFM, a kind of SPM) equipped with a sharp probe that detected the infrared light absorption by a material with nanoscale spatial precision [106,107].

Initially, the method required that the sample be placed on an infrared-transparent prism and had a thickness of less than 1  $\mu\text{m}$  [108]. This pioneering configuration increased the spatial resolution and sensitivity of photothermal AFM-based methods from microns to about 100 nm [109]. Then, with the advent of contemporary pulsed optical parametric oscillators and quantum cascade lasers, along with top illumination, it became possible to examine samples on any substrate with increased sensitivity and spatial resolution. As a result of recent advances, AFM-IR has been demonstrated to be capable of acquiring chemical maps and nanoscale resolved spectra at the single-molecule level with a diameter of approximately 10 nm [105,110]. AFM-IR produces an infrared absorption spectrum by measuring the quantity of infrared absorption as a function of wavelength or wavenumber. This spectrum may be used to chemically analyze and even identify unknown materials [111]. By measuring infrared absorption as a function of location, chemical composition maps may be created that depict the geographical distribution of various chemical components [112].

AFM-IR techniques are now being used to study NPs [113]. Analyzed PE and PS nanowires deposited in complete internal reflection mode on the IR-transparent ZnSe prism and obtained a spatial resolution of more than 100 nm [114]. Used AFM-IR to study PLA NPs (<200 nm) directly within a cell without labeling and a typical result is presented in Figure 10. Figure 10 illustrates the technique's potential to an excellent degree. This technique allowed us to photograph the whole cell (Figure 10a), to identify a region of interest within the  $1770\text{ cm}^{-1}$  chemical map (Figure 10b) and to conduct a spectral analysis on a small portion of the image (Figure 10c,d; region indicated with the yellow dashed circle in Figure 10b). They concluded that AFM-IR may be a valuable technique for determining the fate of individual unlabeled NP particles inside cells.

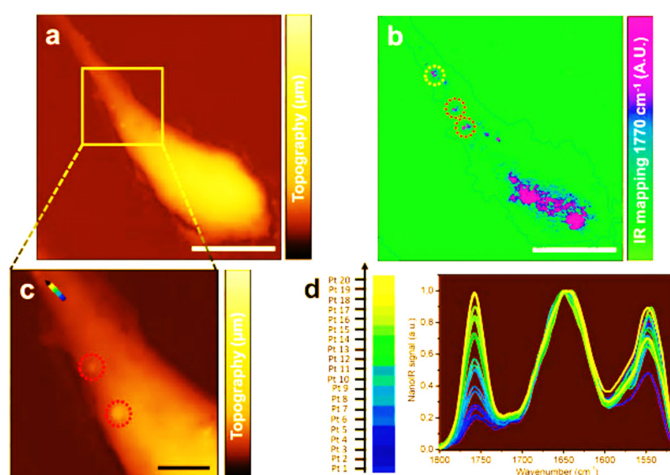


**Figure 10.** Unlabeled imaging of Poly(lactic acid) (PLA) NPs in a cell analyzed by ATM-IR. (a) AFM topography of a THP-1 macrophage (color grading = 0–3  $\mu\text{m}$ ). (b) IR map of the cell at  $1770\text{ cm}^{-1}$ . The selected zone (dashed yellow circle) includes several PLA NPs (color grading = 0–100 A.U.). (c) Zoomed AFM topography showing two intracellular compartments containing NPs (red dashed circles (b,c)). The multicolor arrow represents a row of spectra acquired with a 50 nm step, (d) IR spectra acquired along this line. Ref [114] Reproduced with permission from Pancani et al., Part. Part. Syst. Charact.; published by Wiley-VCH, 2018.

#### 4.3.4. Nanoscale Fourier Transform Infrared Spectroscopy (Nano-FTIR)

Nano-FTIR, also known as scattering-type scanning near-field optical spectroscopy (s-SNOM), is a scanning probe method that may be thought of as a mixture of two techniques: FTIR and s-SNOM. As with s-SNOM, nano-FTIR is based on AFM, in which a sharp tip is lit by an external light source and the tip-scattered light (usually back-scattered) is measured in response to the tip location. Thus, a typical nano-FTIR setup comprises of an AFM, a broadband infrared light source used to illuminate the tip and a Michelson interferometer serving as the Fourier transform spectrometer [115]. The nano-FTIR technique enables the determination of surfaces' broadband infrared absorption spectra with spatial resolutions as low as 10 to 20 nm [116].

The sample stage is positioned in one of the interferometer arms of nano-FTIR, allowing for the simultaneous recording of the amplitude and phase of the observed light (unlike conventional FTIR that normally does not yield phase information). Scanning the tip enables hyperspectral imaging (full spectrum at each pixel in the scanned region) with nanoscale spatial resolution defined by the size of the tip apex. The use of broadband infrared sources allows the collection of continuous spectra, a characteristic of nano-FTIR that distinguishes it from s-SNOM. It has been shown that a single molecule compound may be detected [117] and that a single monolayer can be detected [118]. The recording of infrared spectra as a function of location may be utilized to map the chemical composition of a sample on a nanoscale [119], performing ultrafast infrared spectroscopy on a small scale [120] and studying nanoscale intermolecular coupling [121].

Nano-FTIR has been used for a variety of applications, including the chemical identification of polymers [116,122,123] and nanocomposites [124], onsite characterization of organic thin films, characterization of strain and relaxation in crystalline materials [125], and high-resolution spatial mapping of catalytic reactions [126]. For NPs, [122] studied spherical beads of PMMA with diameter of 30–70 nm on Au-covered Si. Similarly, [116] showed that PMMA NPs samples of diameter 20 nm may be chemically analyzed by Nano-FTIR. Ref. [123] recently shown the applicability of a library-based search for the identification of various polymers identified by nano-FTIR utilizing commercial and open source analytic tools (siMPle). It was discovered that this technique can properly identify polymer samples that have weathered in the environment without previous cleaning,

opening up a broad range of applications for the identification and characterization of different polymer materials [8].

#### 4.3.5. Pyrolysis-Gas Chromatography-Mass Spectrometry (Pyr-GC/MS)

Pyrolysis-gas chromatography-mass spectrometry is a technique for chemical analysis in which a sample is heated to breakdown, resulting in the formation of smaller molecules that are separated and identified using gas chromatography and mass spectrometry [9]. Recently, NPs of less than 1 nm in size, referred to as plastics, were discovered in bulk samples from the North Atlantic Subtropical Gyre and identified using Pyr-GC/MS and statistical methods [11]. A cloud-point extraction (CPE) method based on the triton X-45 (TX-45) was used by Zhou [127] to preconcentrate trace NPs in ambient water. Then, Pyr-GC/MS was used to identify the NPs as PS and PMMA, without altering their original shape and sizes [128]. Davranche [128] applied Pyr-GC/MS on sand water extracts from coast exposed to the North Atlantic Gyre to identify the PS and PVC NPs in the sample. However, because of the low concentrations of NPs in comparison to the OM, there are challenges in using this technique [129]. Ref. [129] identified PP and PS by Py-GC/MS and investigated potential interferences with environmental matrices by spiking NPs in different organic matter suspensions (e.g., algae, soil natural organic matter and soil humic acid). Depending on the nature of the polymers and the amount of OM present, two distinct and complimentary methods were devised. While PP NPs may be detected immediately in complicated material, PS NPs need a preparatory treatment (via the use of H<sub>2</sub>O<sub>2</sub> and ultraviolet radiation) before they can be discovered. The suggested methods offer up new opportunities for the detection and identification of NPs in environmental matrices such as soil, dust and biota, as well as in biological samples.

#### 4.3.6. Thermal Desorption-Gas Chromatography-Mass Spectrometry (TD-GC/MS)

Thermal desorption (TD) is a method in which materials are heated in order to cause adsorbed chemicals to be released as volatile molecules [2]. Thermal desorption analysis necessitates the direct entrance of a tiny quantity of a sample into a sample tube without the need for any pre-treatment, as well as the use of an inert carrier gas to pass through the volatile sample components and into a cooled trap. The trap is then quickly heated in order to desorb the concentrated volatile chemicals onto a gas chromatographic column, where they may be separated and identified using mass spectrometry once they have been detected and identified [130]. When used in conjunction with a fully automated system, the thermal desorption-gas chromatography-mass spectrometry (TD-GC/MS) method may offer consistent and reliable screening of challenging samples such as food, beverages, soil samples, or cosmetics samples. The method has been applied in the study small MPs [130,131].

TD-GC/MS can be combined with Pyr-GC/MS (i.e., TD-GC/MS + Pyr-GC/MS = TD-Pyr-GC/MS) and be used for NPs analysis. In this method, adsorbed chemicals are first desorbed from the particle by TD and then the polymer is broken by pyrolysis. Both particle treatment methods are connected directly to the same GC-MS equipment, which analyzes desorbed molecules and pyrolysis products, respectively (Figure 11). With this technique, it is possible to identify both the sorbed organic compounds as well as the kind of polymer in a single analytical setting [132]. Recently applied this method for evaluating PS NPs (78 nm) exposed to trace organic chemicals (phenanthrene,  $\alpha$ -cypermethrin and triclosan). The resultant chromatograms and pyrograms of the different polymers were separated based on the distinctive pieces of the polymer in question. Figure 12 shows instances of PS chromatograms and pyrograms as illustrations. For the di- and trimer in TD (Figure 12a) and Pyr (Figure 12b), they were retrieved from the corresponding structures. The pyrogram shown in Figure 12a shows that PS NP particles (78 nm) are already broken into the di- and trimer phases in the TD, indicating that they are already in the process of fragmentation. In Figure 12b, the pyrogram is shown in comparison to the di- and trimer of the PS NP particle, respectively.

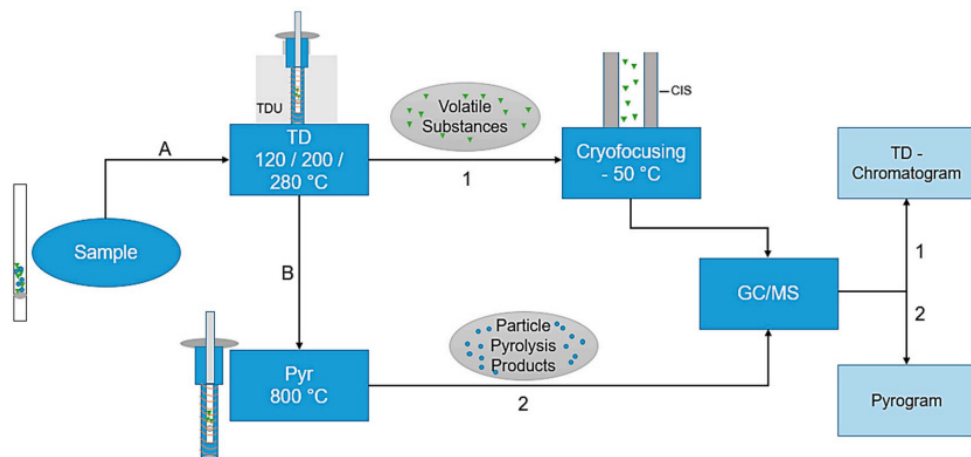


**Figure 11.** TD-Pyr-GC/MS analysis flowchart. To begin, the sample is thermodesorbed (120–280 °C), desorbing volatile compounds and cryofocusing them in the Cooled Injections System (CIS) at 50 °C. Following that, the sample is transferred to a GC column for MS analysis (TD-GC/MS). The identical sample (B) is then pyrolyzed at 800 °C and analyzed by GC/MS (Pyr-GC/MS). The TD-chromatogram and the pyrogram are used to conduct the assessments. Ref [132] Reproduced with permission from Reichel et al., *Molecule*; published by MDPI, 2020.

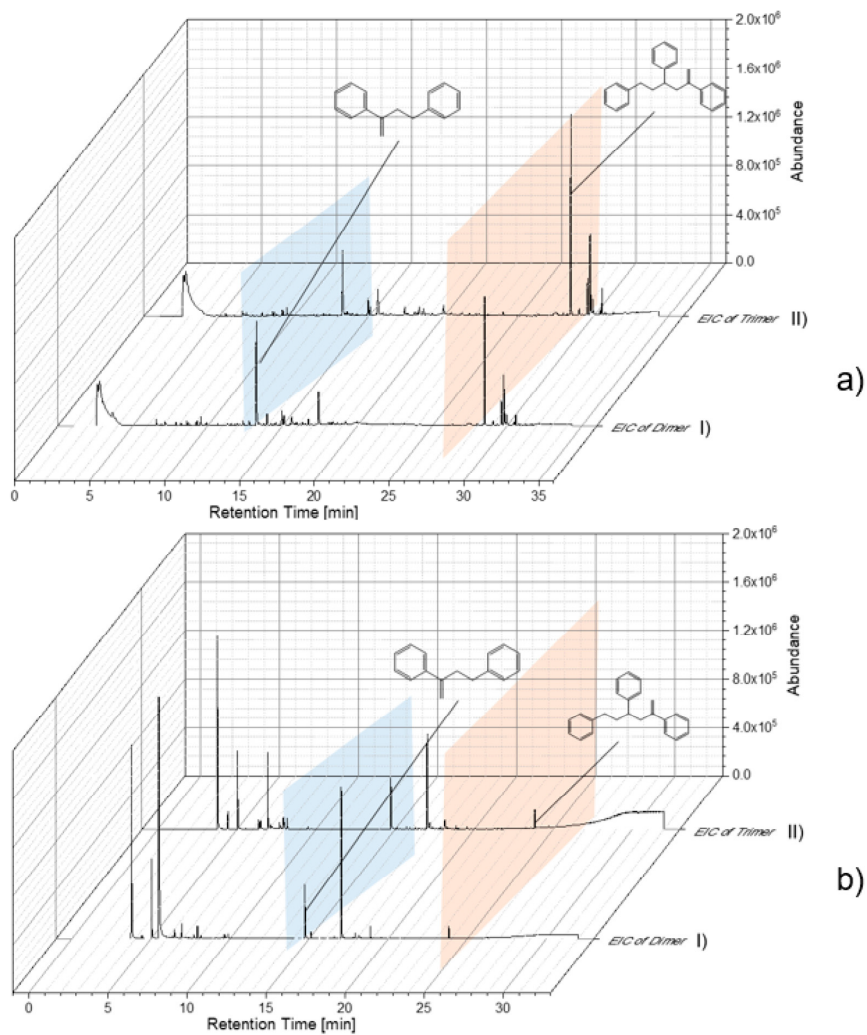


**Figure 12.** Chromatogram/pyrogram analysis of PS 78-nm particles using extracted-ion chromatography (EIC) for dimer (I) and trimer (II): (a) TD-chromatogram (TD-GC/MS), (b) pyrogram (Pyr-GC/MS). Ref [132] Reproduced with permission from Reichel et al., *Molecule*; published by MDPI, 2020.

#### 4.3.7. Thermal Extraction Desorption Gas Chromatography Mass Spectrometry (TED-GC/MS)

The TED-GC-MS technique is based on thermal extraction/pyrolysis of the material on the TGA balance within the TGA furnace, followed by solid phase extraction of complicated volatile hydrocarbons released at elevated temperatures [133,134]. The solid-phase adsorber is then transported to the TD-GC/MS analytical instrument in the second stage. The polymer breakdown markers are thermally desorbed in the introduction system and evaluated by GC/MS for polymer identification and (semi)-quantification. It is possible to analyze bigger samples (15 to 25 mg or more) using TED-GC/MS, resulting in a more representative sample and reducing or eliminating the need to collect repeated samples [135].

This method is now being developed for NPs analysis in complex environmental samples [136,137], but has not been applied to real-life samples. When it comes to automation and improved sample throughput without the need for an extra sample preparation step, TED-GC/MS excels. It may also be used to perform repeatable automated analysis of polymer breakdown processes [135]. Another benefit of TED-GC/MS is its capacity to identify particles of various sizes in the sample, as long as the limit of detection is not surpassed by the instrument [136]. The major disadvantages of utilizing TED-GC-MS are comparable to those of using Pyr-GC/MS, with a focus on the complicated data interpretation, expensive and time-consuming technique development and the lack of the ability to do particle-by-particle analysis on the samples [135].

#### 4.3.8. Thermal Desorption-Proton Transfer Reaction-Mass Spectrometry (TD-PTR-MS)

Mass spectrometry with proton transfer reaction (PTR-MS) is an analytical chemistry method that utilizes gas phase hydronium reagent ions that are generated in an ion source to determine the composition of a sample [138]. Drift tubes are directly linked to an ion source in a PTR-MS apparatus, which allows for faster analysis. PTR-MS equipment that is commercially available has a reaction time of about 100 ms and achieves a detection limit in the single digit pptv or even ppqv range [138]. This technique is widely used in the analysis of various complex organic mixtures in the environment [139,140]. The combination of high sensitivity and excellent mass resolution of the TD-PTR-MS technique is a unique strength of the technology [141]. Whereas the latter enables for chemical identification of compounds down to the level of their chemical formula, high sensitivity gives quantitative information on low-concentrated organics. Furthermore, since the sample quantities needed are modest, this technique is well suited for high-throughput testing. One study recently applied TD-PTR/MS in the analysis of PET and PVC NPs in snow samples [12]. As a result, they concluded that the method's high sensitivity represents a significant advance in the area, bridging the methodological gap between chemical characterization and quantification at the nanogram scale.

In spite of this, numerous unknowns remain as a result of the absence of NPs standards of various kinds and sizes. Due to this, it is still necessary to provide a comprehensive description of the loss during filtering, the weathering impact of NPs, oxidation changes and degrading procedures. Further research is required to combine the accuracy of this sensitive chemical characterization method with a technique that would provide information about the size and shape of the particles, allowing for a more comprehensive evaluation of the potential damage of nanoparticles (NPs) in the environment [12].

#### 4.3.9. Matrix-Assisted Laser Desorption/Ionization-Time of Flight Mass Spectrometry (MALDI-TOF MS)

MALDI-TOF MS is a potent identification method for the ionization and detection of intact molecules with large molecular weights [142]. It is made up of three critical components: ionization, duration of flight (separation) and detection [143]. Pipette the samples onto a stainless-steel sample plate, which is then evaporated and ionized to produce the ionization components. The charged analytes are then separated at various voltages and identified using mass spectrometry based on their mass to charge ratio ( $m/z$ ).

With advantages such as ease of use, high sensitivity, high throughput and reproducible results, the MALDI-TOF MS method has gained increasing attention for the analysis of emerging pollutants in environmental and biological samples [144], and more recently, for the detection of NPs in environmental samples [143,144]. Wu [143] applied this method in analyzing PS and PET particles in the range of 200 to 400 nm. The polymers were soft ionized and then taken away by the vaporized matrix as a result of the laser energy absorption. They are introduced into the TOF and separated according to their  $m/z$ . Finally, the MS findings may be retrieved for additional examination, including the repeating unit mass, end groups and molecular formula, which are crucial for identifying NPs, particularly those that have undergone aging or degradation processes. Lin [144] using a thermally enhanced MALDI-TOF MS was able to analyze particles less than 100 nm. The protocol for this method is presented in Figure 13. However, there are limitations to the technique's ability to provide the NPs' distribution, size and shape.

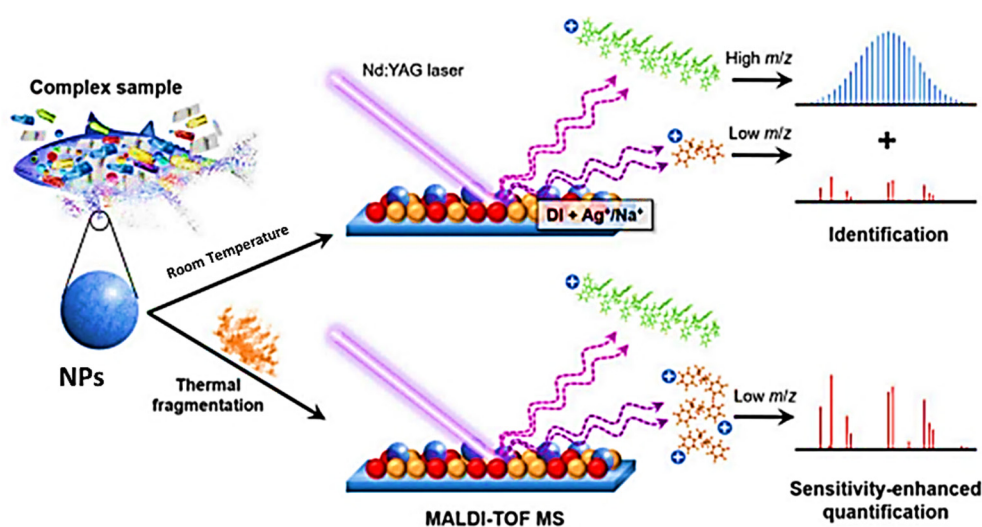


**Figure 13.** Schematic representation of the protocol for thermally improved detection and quantification of PS NPs by MALDI-TOF MS. Ref [144] Reproduced with permission from Lin et al., *Talanta*; published by Elsevier, 2019.

## 5. Conclusions and Future Perspectives

Humans have increased their production and usage of plastic in recent decades, to the point that it has become the most damaging humanmade waste in the environment to date. However, knowledge on the existence of NPs in various environmental matrices, such as their impact on human health and rapid monitoring, is lacking. We discussed the various methods for detecting and characterizing NPs in environmental samples in this review, emphasizing their benefits and disadvantages. The method/combination of techniques used must be carefully assessed in relation to the research topic being addressed. At the moment, there is no one-size-fits-all technique for identifying and characterizing samples. To this aim, we suggest mixing several methods in order to maximize each technique's particular benefits. For instance, correlative microscopy methods may be used to combine the chemical specificity of spectroscopic techniques with the high resolution of electron microscopy. Examining different areas may be beneficial in developing approaches that include a variety of methodologies. Nanoscale separations and analysis, for example, are common in areas such as cellular and molecular biology. Borrowing methodological ideas from these areas may aid in the creation of novel methods to address unresolved issues in NPs research.

To close the existing knowledge gaps, additional research is urgently needed, with a particular emphasis on: (1) careful optimization of sample collection and preparation strategies; and (2) development and optimization of MS-based analytical methods to increase their capabilities and decrease their size detection limits. While further study

in this area is undoubtedly necessary, the current knowledge in NPs sample techniques and recent advances in MS-based analytical approaches offer tremendous promise for proper characterization. However, some of the techniques (used from sample preparation to analysis) involves thermal or combustion processes, which may result in the release of certain pollutants. As a result, some NP methods are not especially “sustainable” or “green”. This may be because NP detection in environmental samples is a relatively new development, many techniques are still in their infancy, there is a worldwide lack of standardization and many efficiency issues and implementation is still a work in progress.

**Author Contributions:** Conceptualization, C.E.E.; methodology, C.E.E.; validation, C.E.E., Q.W., formal analysis, C.E.E., Q.W.; resources contribution, Q.W.; data curation, C.E.E., Q.W.; writing—original draft preparation, C.E.E.; writing—review and editing, C.E.E., Q.W., S.L., K.X., T.C., M.A.H.C. and W.W.; supervision, Q.W., funding acquisition, Q.W. All authors have read and agreed to the published version of the manuscript.

**Funding:** Funding: This study was partially supported by the Special Funds for Innovative Area Research (No.20120015, FY 2008-FY2012) and Basic Research (B) (No. 24310005, FY2012-FY2014; No.18H03384, FY2017 FY2020) of Grant-in-Aid for Scientific Research of Japanese Ministry of Education, Culture, Sports, Science and Technology (MEXT) and the Steel Foundation for Environmental Protection Technology of Japan (No. C-33, FY 2015-FY 2017).

**Institutional Review Board Statement:** Not available.

**Informed Consent Statement:** Not available.

**Data Availability Statement:** Not available.

**Conflicts of Interest:** There are no conflict of interest to declare.

## References

1. Enyoh, C.E.; Ohiagu, F.O.; Verla, A.W.; Wang, Q.; Shafea, L.; Verla, E.N.; Isiuku, B.O.; Chowdhury, T.; Ibe, F.C.; Chowdhury, A.H. “Plasti-remediation”: Advances in the potential use of environmental plastics for pollutant removal. *Environ. Technol. Innov.* **2021**, *23*, 101791. [[CrossRef](#)]
2. Nguyen, B.; Claveau-Mallet, D.; Hernandez, L.M.; Xu, E.G.; Farner, J.M.; Tufenkji, N. Separation and analysis of microplastics and nanoplastics in complex environmental samples. *Acc. Chem. Res.* **2019**, *52*, 858–866. [[CrossRef](#)]
3. Enyoh, C.E.; Verla, A.W.; Qingyue, W.; Ohiagu, F.O.; Chowdhury, A.H.; Enyoh, E.C.; Chowdhury, T.; Verla, E.N.; Chinwendu, U.P. An overview of emerging pollutants in air: Method of analysis and potential public health concern from human environmental exposure. *Trends Environ. Anal. Chem.* **2020**, *28*, e00107. [[CrossRef](#)]
4. Gigault, J.; Pedrono, B.; Maxit, B.; Ter Halle, A. Marine plastic litter: The unanalyzed nano-fraction. *Environ. Sci. Nano* **2016**, *3*, 346–350. [[CrossRef](#)]
5. Lambert, S.; Wagner, M. Characterisation of nanoplastics during the degradation of polystyrene. *Chemosphere* **2016**, *145*, 265–268. [[CrossRef](#)] [[PubMed](#)]
6. Dawson, A.L.; Kawaguchi, S.; King, C.; Townsend, K.; King, R.; Huston, W.; Nash, S.B. Turning microplastics into nanoplastics through digestive fragmentation by Antarctic krill. *Nat. Commun.* **2018**, *9*, 1001. [[CrossRef](#)]
7. Wang, Q.; Enyoh, C.E.; Chowdhury, T.; Chowdhury, A.H. Analytical techniques, occurrence and health effects of micro and nano plastics deposited in street dust. *Int. J. Environ. Anal. Chem.* **2020**, *1*–19. [[CrossRef](#)]
8. Ivleva, N.P. Chemical analysis of microplastics and nanoplastics: Challenges, advanced methods, and perspectives. *Chem. Rev.* **2021**, *121*, 11886–11936. [[CrossRef](#)]
9. Verla, A.W.; Enyoh, C.E.; Verla, E.N.; Nwarnorh, K.O. Microplastic–toxic chemical interaction: A review study on quantified levels, mechanism and implication. *SN Appl. Sci.* **2019**, *1*, 1400. [[CrossRef](#)]
10. Picó, Y.; Barceló, D. Analysis of microplastics and nanoplastics: How green are the methodologies used? *Curr. Opin. Green Sustain. Chem.* **2021**, *31*, 100503. [[CrossRef](#)]
11. Ter Halle, A.; Jeanneau, L.; Martignac, M.; Jardé, E.; Pedrono, B.; Brach, L.; Gigault, J. Nanoplastic in the North Atlantic Subtropical Gyre. *Environ. Sci. Technol.* **2017**, *51*, 13689–13697. [[CrossRef](#)]
12. Materić, D.; Kasper-Giebl, A.; Kau, D.; Anten, M.; Greilinger, M.; Ludewig, E.; Van Sebille, E.; Röckmann, T.; Holzinger, R. Micro- and nanoplastics in alpine snow: A new method for chemical identification and (semi)quantification in the nanogram range. *Environ. Sci. Technol.* **2020**, *54*, 2353–2359. [[CrossRef](#)] [[PubMed](#)]
13. Wahl, A.; Le Juge, C.; Davranche, M.; El Hadri, H.; Grassl, B.; Reynaud, S.; Gigault, J. Nanoplastic occurrence in a soil amended with plastic debris. *Chemosphere* **2021**, *262*, 127784. [[CrossRef](#)]
14. Hernandez, L.M.; Yousefi, N.; Tufenkji, N. Are there nanoplastics in your personal care products? *Environ. Sci. Technol. Lett.* **2017**, *4*, 280–285. [[CrossRef](#)]

15. Schwaferts, C.; Niessner, R.; Elsner, M.; Ivleva, N.P. Methods for the analysis of submicrometer- and nanoplastic particles in the environment. *TrAC Trends Anal. Chem.* **2019**, *112*, 52–65. [[CrossRef](#)]
16. Hildebrandt, L.; Mitrano, D.; Zimmermann, T.; Pröfrock, D. A nanoplastic sampling and enrichment approach by continuous flow centrifugation. *Front. Environ. Sci.* **2020**, *8*, 89. [[CrossRef](#)]
17. Delgado-Gallardo, J.; Sullivan, G.L.; Esteban, P.; Wang, Z.; Arar, O.; Li, Z.; Watson, T.M.; Sarp, S. From sampling to analysis: A critical review of techniques used in the detection of micro- and nanoplastics in aquatic environments. *ACS ES&T Water* **2021**, *1*, 748–764. [[CrossRef](#)]
18. Nuelle, M.-T.; Dekiff, J.H.; Remy, D.; Fries, E. A new analytical approach for monitoring microplastics in marine sediments. *Environ. Pollut.* **2014**, *184*, 161–169. [[CrossRef](#)]
19. Wirnkör, V.A.; Ebere, E.C.; Ngozi, V.E. Microplastics, an emerging concern: A review of analytical techniques for detecting and quantifying microplastics. *Anal. Methods Environ. Chem. J.* **2019**, *2*, 13–30. [[CrossRef](#)]
20. Hernandez, L.M.; Xu, E.G.; Larsson, H.C.E.; Tahara, R.; Maisuria, V.B.; Tufenkji, N. Plastic teabags release billions of microparticles and nanoparticles into tea. *Environ. Sci. Technol.* **2019**, *53*, 12300–12310. [[CrossRef](#)]
21. Erni-cassola, G.; Gibson, M.I.; Thompson, R.C.; Christie-Oleza, J.A. Lost, but found with Nile Red: A novel method to detecting and quantifying small microplastics (1 mm to 20  $\mu$ m) in environmental samples. *Environ. Sci. Technol.* **2017**, *51*, 13641–13648. [[CrossRef](#)] [[PubMed](#)]
22. Abdelrasoul, A.; Doan, H.; Lohi, A.; Cheng, C.-H. The influence of aggregation of latex particles on membrane fouling attachments & ultrafiltration performance in ultrafiltration of latex contaminated water and wastewater. *J. Environ. Sci.* **2017**, *52*, 118–129. [[CrossRef](#)]
23. Zhou, X.-X.; Lai, Y.-J.; Liu, R.; Li, S.-S.; Xu, J.-W.; Liu, J.-F. Polyvinylidene fluoride micropore membranes as solid-phase extraction disk for preconcentration of nanoparticulate silver in environmental waters. *Environ. Sci. Technol.* **2017**, *51*, 13816–13824. [[CrossRef](#)] [[PubMed](#)]
24. Pitt, J.A.; Trevisan, R.; Massarsky, A.; Kozal, J.S.; Levin, E.D.; Di Giulio, R.T. Maternal transfer of nanoplastics to offspring in zebrafish (*Danio rerio*): A case study with nanopolystyrene. *Sci. Total. Environ.* **2018**, *643*, 324–334. [[CrossRef](#)]
25. Mintenig, S.M.; Bäuerlein, P.S.; Koelmans, A.A.; Dekker, S.C.; Van Wezel, A.P. Closing the gap between small and smaller: Towards a framework to analyse nano- and microplastics in aqueous environmental samples. *Environ. Sci. Nano* **2018**, *5*, 1640–1649. [[CrossRef](#)]
26. Majedi, S.M.; Lee, H.K. Recent advances in the separation and quantification of metallic nanoparticles and ions in the environment. *TrAC Trends Anal. Chem.* **2016**, *75*, 183–196. [[CrossRef](#)]
27. Käppler, A.; Windrich, F.; Löder, M.G.J.; Malanin, M.; Fischer, D.; Labrenz, M.; Eichhorn, K.-J.; Voit, B. Identification of microplastics by FTIR and Raman microscopy: A novel silicon filter substrate opens the important spectral range below 1300  $\text{cm}^{-1}$  for FTIR transmission measurements. *Anal. Bioanal. Chem.* **2015**, *407*, 6791–6801. [[CrossRef](#)]
28. Vauthier, C.; Bouchemal, K. Methods for the preparation and manufacture of polymeric nanoparticles. *Pharm. Res.* **2009**, *26*, 1025–1058. [[CrossRef](#)]
29. Mendes, A. Lab Basics, Laboratory Techniques, Science. Ultracentrifugation Basics and Applications. 2020. Available online: <https://conductscience.com/ultracentrifugation-basics-and-applications/> (accessed on 16 October 2021).
30. Laborda, F.; Bolea, E.; Cepriá, G.; Gómez, M.T.; Jiménez, M.S.; Perez-Arantequi, J.; Castillo, J.R. Detection, characterization and quantification of inorganic engineered nanomaterials: A review of techniques and methodological approaches for the analysis of complex samples. *Anal. Chim. Acta* **2016**, *904*, 10–32. [[CrossRef](#)]
31. Staff, R.H.; Landfester, K.; Crespy, D. Recent advances in the emulsion solvent evaporation technique for the preparation of nanoparticles and nanocapsules. *Adv. Polym. Sci.* **2013**, *262*, 329–344. [[CrossRef](#)]
32. Atkin, R.; Davies, P.; Hardy, A.J.; Vincent, B. Preparation of aqueous core/polymer shell microcapsules by internal phase separation. *Macromolecules* **2004**, *37*, 7979–7985. [[CrossRef](#)]
33. Urbaniak, T.; Musiał, W. Influence of solvent evaporation technique parameters on diameter of submicron lamivudine-poly- $\epsilon$ -caprolactone conjugate particles. *Nanomaterials* **2019**, *9*, 1240. [[CrossRef](#)]
34. Mehta, M.; Saurabh, S.; Parijat, P.; Mandeep, D. Solvent evaporation technique: An innovative approach to increase gastric retention. *Int. J. Adv. Sci. Res.* **2016**, *1*, 60–67.
35. Zhang, H.; Lyden, D. Asymmetric-flow field-flow fractionation technology for exomere and small extracellular vesicle separation and characterization. *Nat. Protoc.* **2019**, *14*, 1027–1053. [[CrossRef](#)] [[PubMed](#)]
36. Baalousha, M.; Stolpe, B.; Lead, J. Flow field-flow fractionation for the analysis and characterization of natural colloids and manufactured nanoparticles in environmental systems: A critical review. *J. Chromatogr. A* **2011**, *1218*, 4078–4103. [[CrossRef](#)]
37. Correia, M.; Loeschner, K. Detection of nanoplastics in food by asymmetric flow field-flow fractionation coupled to multi-angle light scattering: Possibilities, challenges and analytical limitations. *Anal. Bioanal. Chem.* **2018**, *410*, 5603–5615. [[CrossRef](#)] [[PubMed](#)]
38. Mowla, M.; Shakiba, S.; Louie, S.M. Selective quantification of nanoplastics in environmental matrices by asymmetric flow field—flow fractionation with total organic carbon detection. *Chem. Commun.* **2021**, 1–30. [[CrossRef](#)] [[PubMed](#)]
39. Klein, S.; Dimzon, I.K.; Eubeler, J.; Knepper, T.P. Analysis, occurrence, and degradation of microplastics in the aqueous environment. In *Freshwater Microplastics: Emerging Environmental Contaminants?* Wagner, M., Lambert, S., Eds.; Springer: Cham, Switzerland, 2018; pp. 51–67.

40. Williams, P.S.; Carpino, F.; Zborowski, M. Characterization of magnetic nanoparticles using programmed quadrupole magnetic field-flow fractionation. *Philos. Trans. R. Soc. A Math. Phys. Eng. Sci.* **2010**, *368*, 4419–4437. [CrossRef]
41. Latham, A.H.; Freitas, R.S.; Schiffer, P.; Williams, M.E. Capillary magnetic field flow fractionation and analysis of magnetic nanoparticles. *Anal. Chem.* **2005**, *77*, 5055–5062. [CrossRef]
42. von der Kammer, F.; Legros, S.; Hofmann, T.; Larsen, E.H.; Loeschner, K. Separation and characterization of nanoparticles in complex food and environmental samples by field-flow fractionation. *TrAC Trends Anal. Chem.* **2011**, *30*, 425–436. [CrossRef]
43. Botello, I.; Borrull, F.; Calull, M.; Aguilar, C.; Somsen, G.W.; de Jong, G.J. In-line solid-phase extraction—capillary electrophoresis coupled with mass spectrometry for determination of drugs of abuse in human urine. *Anal. Bioanal. Chem.* **2012**, *403*, 777–784. [CrossRef] [PubMed]
44. Parsons, M.E.M.; McParland, D.; Szklanna, P.B.; Guang, M.H.Z.; O’Connell, K.; O’Connor, H.D.; McGuigan, C.; Áinle, F.N.; McCann, A.; Maguire, P.B. A protocol for improved precision and increased confidence in nanoparticle tracking analysis concentration measurements between 50 and 120 nm in biological fluids. *Front. Cardiovasc. Med.* **2017**, *4*, 68. [CrossRef] [PubMed]
45. Voeten, R.L.C.; Ventouri, I.K.; Haselberg, R.; Somsen, G.W. Capillary Electrophoresis: Trends and Recent Advances. *Anal. Chem.* **2018**, *90*, 1464–1481. [CrossRef]
46. Enyoh, C.E.; Isiuku, B.O.; Verla, A.W. Applications of column, paper, thin layer and ion exchange chromatography in purifying samples: Mini review. *SF J. Pharm. Anal. Chem.* **2019**, *2*, 1–6.
47. Gerber, F.; Krummen, M.; Potgeter, H.; Roth, A.; Siffrin, C.; Spoendlin, C. Practical aspects of fast reversed-phase high-performance liquid chromatography using 3 µm particle packed columns and monolithic columns in pharmaceutical development and production working under current good manufacturing practice. *J. Chromatogr. A* **2004**, *1036*, 127–133. [CrossRef]
48. Soto-Alvaredo, J.; Montes-Bayón, M.; Bettmer, J. Speciation of silver nanoparticles and silver(I) by reversed-phase liquid chromatography coupled to ICPMS. *Anal. Chem.* **2013**, *85*, 1316–1321. [CrossRef]
49. Sötebier, C.A.; Weidner, S.M.; Jakubowski, N.; Panne, U.; Bettmer, J. Separation and quantification of silver nanoparticles and silver ions using reversed phase high performance liquid chromatography coupled to inductively coupled plasma mass spectrometry in combination with isotope dilution analysis. *J. Chromatogr. A* **2016**, *1468*, 102–108. [CrossRef]
50. Majors, R.E. Fast and ultrafast HPLC on sub-2 µm porous particles—Where do we go from here? *LCGC Eur.* **2006**, *19*, 352–362.
51. Zhou, X.-X.; Liu, R.; Liu, J.-F. Rapid chromatographic separation of dissolvable Ag(I) and silver-containing nanoparticles of 1–100 nanometer in antibacterial products and environmental waters. *Environ. Sci. Technol.* **2014**, *48*, 14516–14524. [CrossRef] [PubMed]
52. Kumar, P.; Mina, U. *Fundamentals and Techniques of Biophysics and Molecular Biology*; Pathfinder Publication: Greater Noida, India, 2016.
53. Tiede, K.; Boxall, A.B.A.; Tiede, D.; Tear, S.P.; David, H.; Lewis, J. A robust size-characterisation methodology for studying nanoparticle behaviour in ‘real’ environmental samples, using hydrodynamic chromatography coupled to ICP-MS. *J. Anal. At. Spectrom.* **2009**, *24*, 964–972. [CrossRef]
54. Critchley, L. Comparing Optical and Electron Microscopy for Nanomaterial Analysis. AZoNano. 2019. Available online: <https://www.azonano.com/article.aspx?ArticleID=5339> (accessed on 11 October 2021).
55. Attota, R.; Kavuri, P.P.; Kang, H.; Kasica, R.; Chen, L. Nanoparticle size determination using optical microscopes. *Appl. Phys. Lett.* **2014**, *105*, 163105. [CrossRef]
56. Chae, Y.; Kim, D.; Kim, S.W.; An, Y.-J. Trophic transfer and individual impact of nano-sized polystyrene in a four-species freshwater food chain. *Sci. Rep.* **2018**, *8*, 1–11. [CrossRef]
57. Khoshnamvand, M.; Hanachi, P.; Ashtiani, S.; Walker, T.R. Toxic effects of polystyrene nanoplastics on microalgae *Chlorella vulgaris*: Changes in biomass, photosynthetic pigments and morphology. *Chemosphere* **2021**, *280*, 130725. [CrossRef]
58. Gunkel, M.; Erdel, F.; Rippe, K.; Lemmer, P.; Kaufmann, R.; Hörmann, C.; Amberger, R.; Cremer, C. Dual color localization microscopy of cellular nanostructures. *Biotechnol. J.* **2009**, *4*, 927–938. [CrossRef]
59. Cole, M.; Lindeque, P.; Fileman, E.; Halsband, C.; Goodhead, R.; Moger, J.; Galloway, T.S. Microplastic ingestion by zooplankton. *Environ. Sci. Technol.* **2013**, *47*, 6646–6655. [CrossRef]
60. Mariano, S.; Tacconi, S.; Fidaleo, M.; Rossi, M.; Dini, L. Micro and nanoplastics identification: Classic methods and innovative detection techniques. *Front. Toxicol.* **2021**, *3*, 2. [CrossRef]
61. Lee, K.W.; Shim, W.J.; Kwon, O.Y.; Kang, J.H. Size-dependent effects of micro polystyrene particles in the marine copepod *tigriopus japonicus*. *Environ. Sci. Technol.* **2013**, *47*, 11278–11283. [CrossRef] [PubMed]
62. Li, L.; Zhou, Q.; Yin, N.; Tu, C.; Luo, Y. Uptake and accumulation of microplastics in an edible plant. *Chin. Sci. Bull.* **2019**, *64*, 928–934. [CrossRef]
63. Andreozzi, P.; Martinelli, C.; Carney, R.; Carney, T.M.; Stellacci, F. Erythrocyte incubation as a method for free-dye presence determination in fluorescently labeled nanoparticles. *Mol. Pharm.* **2012**, *10*, 875–882. [CrossRef] [PubMed]
64. Lee, Y.K.; Murphy, K.R.; Hur, J. Fluorescence signatures of dissolved organic matter leached from microplastics: Polymers and additives. *Environ. Sci. Technol.* **2020**, *54*, 11905–11914. [CrossRef] [PubMed]
65. Dini, L.; Panzarini, E.; Mariano, S.; Passeri, D.; Reggente, M.; Rossi, M.; Vergallo, C. Microscopies at the nanoscale for nano-scale drug delivery systems. *Curr. Drug Targets* **2015**, *16*, 1512–1530. [CrossRef] [PubMed]
66. Nemmar, A.; Al-Maskari, S.; Ali, B.H.; Al-Amri, I. Cardiovascular and lung inflammatory effects induced by systemically administered diesel exhaust particles in rats. *Am. J. Physiol. Cell. Mol. Physiol.* **2007**, *292*, L664–L670. [CrossRef] [PubMed]

67. Takenaka, S.; Karg, E.; Kreyling, W.; Lentner, B.; Möller, W.; Behnke-Semmler, M.; Jennen, L.; Walch, A.; Michalke, B.; Schramel, P.; et al. Distribution pattern of inhaled ultrafine gold particles in the rat lung. *Inhal. Toxicol.* **2006**, *18*, 733–740. [[CrossRef](#)] [[PubMed](#)]
68. Pulskamp, K.; Diabaté, S.; Krug, H.F. Carbon nanotubes show no sign of acute toxicity but induce intracellular reactive oxygen species in dependence on contaminants. *Toxicol. Lett.* **2007**, *168*, 58–74. [[CrossRef](#)] [[PubMed](#)]
69. Zepp, R.; Ruggiero, E.; Acrey, B.; Davis, M.J.B.J.B.; Han, C.; Hsieh, H.-S.; Vilsmeier, K.; Wohlleben, W.; Sahle-Demessie, E. Fragmentation of polymer nanocomposites: Modulation by dry and wet weathering, fractionation, and nanomaterial filler. *Environ. Sci. Nano* **2020**, *7*, 1742–1758. [[CrossRef](#)]
70. Sun, X.; Chen, B.; Li, Q.; Liu, N.; Xia, B.; Zhu, L.; Qu, K. Toxicities of polystyrene nano- and microplastics toward marine bacterium *Halomonas alkaliphila*. *Sci. Total. Environ.* **2018**, *642*, 1378–1385. [[CrossRef](#)]
71. Song, C.; Liu, Z.; Wang, C.; Li, S.; Kitamura, Y. Different interaction performance between microplastics and microalgae: The bio-elimination potential of *Chlorella* sp. L38 and *Phaeodactylum tricornutum* MASCC-0025. *Sci. Total. Environ.* **2020**, *723*, 138146. [[CrossRef](#)]
72. Wang, S.; Liu, M.; Wang, J.; Huang, J.; Wang, J. Polystyrene nanoplastics cause growth inhibition, morphological damage and physiological disturbance in the marine microalga *Platymonas helgolandica*. *Mar. Pollut. Bull.* **2020**, *158*, 111403. [[CrossRef](#)]
73. Hazeem, L.J.; Yesilay, G.; Bououdina, M.; Perna, S.; Cetin, D.; Suludere, Z.; Barras, A.; Boukherroub, R. Investigation of the toxic effects of different polystyrene micro- and nanoplastics on microalgae *Chlorella vulgaris* by analysis of cell viability, pigment content, oxidative stress and ultrastructural changes. *Mar. Pollut. Bull.* **2020**, *156*, 111278. [[CrossRef](#)]
74. Mühlfeld, C.; Rothen-Rutishauser, B.; Vanhecke, D.; Blank, F.; Gehr, P.; Ochs, M. Visualization and quantitative analysis of nanoparticles in the respiratory tract by transmission electron microscopy. *Part. Fibre Toxicol.* **2007**, *4*, 11. [[CrossRef](#)]
75. Havrdova, M.; Polakova, K.; Skopalik, J.; Vujtek, M.; Mokdad, A.; Homolkova, M.; Tucek, J.; Nebesarova, J.; Zboril, R. Field emission scanning electron microscopy (FE-SEM) as an approach for nanoparticle detection inside cells. *Micron* **2014**, *67*, 149–154. [[CrossRef](#)] [[PubMed](#)]
76. Zheng, J.; Nagashima, K.; Parmiter, D.; de la Cruz, J.; Patri, A.K. SEM x-ray microanalysis of nanoparticles present in tissue or cultured cell thin sections. *Methods Mol. Biol.* **2011**, *697*, 93–99. [[CrossRef](#)]
77. Junoh, H.; Jaafar, J.; Nordin, N.A.H.M.; Ismail, A.F.; Othman, M.H.D.; Rahman, M.A.; Aziz, F.; Yusof, N. Synthetic polymer-based membranes for direct methanol fuel cell (DMFC) applications. In *Synthetic Polymeric Membranes for Advanced Water Treatment, Gas Separation, and Energy Sustainability*; Elsevier: Amsterdam, The Netherlands, 2020; pp. 337–363.
78. Naji, A.; Nuri, M.; Amiri, P.; Niyogi, S. Small microplastic particles (S-MPPs) in sediments of mangrove ecosystem on the northern coast of the Persian Gulf. *Mar. Pollut. Bull.* **2019**, *146*, 305–311. [[CrossRef](#)] [[PubMed](#)]
79. Orasugh, J.T.; Ghosh, S.K.; Chattopadhyay, D. Nanofiber-reinforced biocomposites. In *Fiber-Reinforced Nanocomposites: Fundamentals and Applications*; Elsevier: Amsterdam, The Netherlands, 2020; pp. 199–233.
80. Serem, W.K.; Lusker, K.L.; Garno, J.C. Using scanning probe microscopy to characterize nanoparticles and nanocrystals. In *Encyclopedia of Analytical Chemistry*; Wiley: Hoboken, NJ, USA, 2010.
81. Daniels, S.L.; Ngunjiri, J.N.; Garno, J.C. Investigation of the magnetic properties of ferritin by AFM imaging with magnetic sample modulation. *Anal. Bioanal. Chem.* **2009**, *394*, 215–223. [[CrossRef](#)] [[PubMed](#)]
82. Hermann, R.J.; Gordon, M.J. Nanoscale optical microscopy and spectroscopy using near-field probes. *Annu. Rev. Chem. Biomol. Eng.* **2018**, *9*, 365–387. [[CrossRef](#)]
83. Kuroski, D.; Dazzi, A.; Zenobi, R.; Centrone, A. Infrared and Raman chemical imaging and spectroscopy at the nanoscale. *Chem. Soc. Rev.* **2020**, *49*, 3315–3347. [[CrossRef](#)]
84. Lim, J.; Yeap, S.P.; Che, H.X.; Low, S.C. Characterization of magnetic nanoparticle by dynamic light scattering. *Nanoscale Res. Lett.* **2013**, *8*, 381. [[CrossRef](#)]
85. Berne, B.J.; Pecora, R. *Dynamic Light Scattering: With Applications to Chemistry, Biology, and Physics*; Courier Corporation: Mineloa, NY, USA, 2000.
86. Jans, H.; Liu, X.; Austin, L.; Maes, G.; Huo, Q. Dynamic light scattering as a powerful tool for gold nanoparticle bioconjugation and biomolecular binding studies. *Anal. Chem.* **2009**, *81*, 9425–9432. [[CrossRef](#)]
87. Babick, F. Dynamic light scattering (DLS). Characterization of Nanoparticles. *Micro and Nano Technologies* **2020**, 137–172. [[CrossRef](#)]
88. Munirasu, S.; Nunes, S.P. Porous asymmetric SiO<sub>2</sub>-g-PMMA nanoparticles produced by phase inversion. *J. Mater. Sci.* **2014**, *49*, 7399–7407. [[CrossRef](#)]
89. Altenhoff, M.; Aßmann, S.; Perlitz, J.F.A.; Huber, F.J.T.; Will, S. Soot aggregate sizing in an extended premixed flame by high-resolution two-dimensional multi-angle light scattering (2D-MALS). *Appl. Phys. B* **2019**, *125*, 176. [[CrossRef](#)]
90. Andersson, M.; Wittgren, B.; Wahlund, K.-G. Accuracy in multiangle light scattering measurements for molar mass and radius estimations. model calculations and experiments. *Anal. Chem.* **2003**, *75*, 4279–4291. [[CrossRef](#)] [[PubMed](#)]
91. de Boer, A.; Gjaltema, D.; Hagedoorn, P.; Frijlink, H.W. Characterization of inhalation aerosols: A critical evaluation of cascade impactor analysis and laser diffraction technique. *Int. J. Pharm.* **2002**, *249*, 219–231. [[CrossRef](#)]
92. Martins, F.J.W.A.; Kronenburg, A.; Beyrau, F. Single-shot two-dimensional multi-angle light scattering (2D-MALS) technique for nanoparticle aggregate sizing. *Appl. Phys. B* **2021**, *127*, 51. [[CrossRef](#)]
93. Rawal, S.U.; Patel, M.M. Lipid nanoparticulate systems: Modern versatile drug carriers. In *Lipid Nanocarriers for Drug Targeting*; William Andrew Publishing: Norwich, NY, USA, 2018.

94. Shah, R.; Eldridge, D.; Palombo, E.; Harding, I. *Lipid Nanoparticles: Production, Characterization and Stability*; Springer Science: New York, NY, USA, 2015.
95. Filipe, V.; Hawe, A.; Jiskoot, W. Critical evaluation of nanoparticle tracking analysis (NTA) by nanosight for the measurement of nanoparticles and protein aggregates. *Pharm. Res.* **2010**, *27*, 796–810. [[CrossRef](#)] [[PubMed](#)]
96. Dragovic, R.A.; Gardiner, C.; Brooks, A.S.; Tannetta, D.S.; Ferguson, D.; Hole, P.; Carr, B.; Redman, C.W.; Harris, A.; Dobson, P.J.; et al. Sizing and phenotyping of cellular vesicles using nanoparticle tracking analysis. *Nanomed. Nanotechnol. Biol. Med.* **2011**, *7*, 780–788. [[CrossRef](#)]
97. Ibeto, C.; Enyoh, C.; Ofomatah, A.; Oguejiofor, L.; Okafocha, T.; Okanya, V. Microplastics pollution indices of bottled water from South Eastern Nigeria. *Int. J. Environ. Anal. Chem.* **2021**, 1–20. [[CrossRef](#)]
98. Kawata, S.; Ichimura, T.; Taguchi, A.; Kumamoto, Y. Nano-Raman scattering microscopy: Resolution and enhancement. *Chem. Rev.* **2017**, *117*, 4983–5001. [[CrossRef](#)]
99. Zeng, X.; Han, L.; Singh, S.R.; Liu, H.; Neumüller, R.A.; Yan, D.; Hu, Y.; Liu, Y.; Liu, W.; Lin, X.; et al. Genome-wide RNAi screen identifies networks involved in intestinal stem cell regulation in *Drosophila*. *Cell Rep.* **2015**, *10*, 1226–1238. [[CrossRef](#)]
100. Zhu, L.; Atesang, J.; Dudek, P.; Hecker, M.; Rinderknecht, J.; Ritz, Y.; Geisler, H.; Herr, U.; Geer, R.; Zschech, E. Experimental challenges for approaching local strain determination in silicon by nano-Raman spectroscopy. *Mater. Sci. -Pol.* **2007**, *25*, 19–31.
101. Hartschuh, A.; Beversluis, M.R.; Bouhelier, A.; Novotny, L. Tip-enhanced optical spectroscopy. *Philos. Trans. R. Soc. A: Math. Phys. Eng. Sci.* **2004**, *362*, 807–819. [[CrossRef](#)]
102. Yeo, B.S.; Amstad, E.; Schmid, T.; Stadler, J.; Zenobi, R. Nanoscale probing of a polymer-blend thin film with tip-enhanced Raman spectroscopy. *Small* **2009**, *5*, 952–960. [[CrossRef](#)] [[PubMed](#)]
103. Gillibert, R.; Balakrishnan, G.; Deshoules, Q.; Tardivel, M.; Magazzù, A.; Donato, M.G.; Maragò, O.M.; de La Chapelle, M.L.; Colas, F.J.; Lagarde, F.; et al. Raman tweezers for small microplastics and nanoplastics identification in seawater. *Environ. Sci. Technol.* **2019**, *53*, 9003–9013. [[CrossRef](#)] [[PubMed](#)]
104. Ruggeri, F.S.; Habchi, J.; Chia, S.; Horne, R.I.; Vendruscolo, M.; Knowles, T.P.J. Infrared nanospectroscopy reveals the molecular interaction fingerprint of an aggregation inhibitor with single A $\beta$ 42 oligomers. *Nat. Commun.* **2021**, *12*, 688. [[CrossRef](#)] [[PubMed](#)]
105. Kenkel, S.; Mittal, S.; Bhargava, R. Closed-loop atomic force microscopy-infrared spectroscopic imaging for nanoscale molecular characterization. *Nat. Commun.* **2020**, *11*, 3225. [[CrossRef](#)]
106. Ruggeri, F.S.; Longo, G.; Faggiano, S.; Lipiec, E.; Pastore, A.; Dietler, G. Infrared nanospectroscopy characterization of oligomeric and fibrillar aggregates during amyloid formation. *Nat. Commun.* **2015**, *6*, 7831. [[CrossRef](#)]
107. Dazzi, A.; Prazeres, R.; Glotin, F.; Ortega, J. Analysis of nano-chemical mapping performed by an AFM-based (“AFMIR”) acousto-optic technique. *Ultramicroscopy* **2007**, *107*, 1194–1200. [[CrossRef](#)]
108. Ruggeri, F.S.; Habchi, J.; Cerreta, A.; Dietler, G. AFM-based single molecule techniques: Unraveling the amyloid pathogenic species. *Curr. Pharm. Des.* **2016**, *22*, 3950–3970. [[CrossRef](#)] [[PubMed](#)]
109. Ramer, G.; Ruggeri, F.S.; Levin, A.; Knowles, T.P.J.; Centrone, A. Determination of polypeptide conformation with nanoscale resolution in water. *ACS Nano* **2018**, *12*, 6612–6619. [[CrossRef](#)]
110. Hill, G.A.; Rice, J.H.; Meech, S.R.; Craig, D.Q.M.; Kuo, P.; Vodopyanov, K.; Reading, M. Submicrometer infrared surface imaging using a scanning-probe microscope and an optical parametric oscillator laser. *Opt. Lett.* **2009**, *34*, 431–433. [[CrossRef](#)]
111. Eby, T.; Gundusharma, U.; Lo, M.; Sahagian, K.; Marcott, C.; Kjoller, K. Reverse engineering of polymeric multilayers using AFM-based nanoscale IR spectroscopy and thermal analysis. *Spectrosc. Eur.* **2012**, *24*, 18.
112. Felts, J.R.; Kjoller, K.; Lo, M.; Prater, C.B.; King, W.P. Nanometer-scale infrared spectroscopy of heterogeneous polymer nanostructures fabricated by tip-based nanofabrication. *ACS Nano* **2012**, *6*, 8015–8021. [[CrossRef](#)]
113. Pancani, E.; Mathurin, J.; Bilent, S.; Bernet-Camard, M.-F.; Dazzi, A.; Deniset-Besseau, A.; Gref, R. High-resolution label-free detection of biocompatible polymeric nanoparticles in cells. *Part. Part. Syst. Charact.* **2018**, *35*, 1700457. [[CrossRef](#)]
114. Amarie, S.; Ganz, T.; Keilmann, F. Mid-infrared near-field spectroscopy. *Opt. Express* **2009**, *17*, 21794–21801. [[CrossRef](#)]
115. Huth, F.; Govyadinov, A.; Amarie, S.; Nuansing, W.; Keilmann, F.; Hillenbrand, R. Nano-FTIR absorption spectroscopy of molecular fingerprints at 20 nm spatial resolution. *Nano Lett.* **2012**, *12*, 3973–3978. [[CrossRef](#)]
116. Amenabar, I.; Poly, S.; Nuansing, W.; Hubrich, E.H.; Govyadinov, A.; Huth, F.; Krutokhvostov, R.; Zhang, L.; Knez, M.; Heberle, J.; et al. Structural analysis and mapping of individual protein complexes by infrared nanospectroscopy. *Nat. Commun.* **2013**, *4*, 2890. [[CrossRef](#)] [[PubMed](#)]
117. Xu, X.G.; Rang, M.; Craig, I.M.; Raschke, M.B. Pushing the sample-size limit of infrared vibrational nanospectroscopy: From monolayer toward single molecule sensitivity. *J. Phys. Chem. Lett.* **2012**, *3*, 1836–1841. [[CrossRef](#)]
118. Ugarte, L.; Santamaria-Echart, A.; Mastel, S.; Autore, M.; Hillenbrand, R.; Corcuera, M.A.; Eceiza, A. An alternative approach for the incorporation of cellulose nanocrystals in flexible polyurethane foams based on renewably sourced polyols. *Ind. Crop. Prod.* **2017**, *95*, 564–573. [[CrossRef](#)]
119. Xu, X.G.; Raschke, M.B. Near-field infrared vibrational dynamics and tip-enhanced decoherence. *Nano Lett.* **2013**, *13*, 1588–1595. [[CrossRef](#)] [[PubMed](#)]
120. Pollard, B.; Muller, E.; Hinrichs, K.; Raschke, M.B. Vibrational nano-spectroscopic imaging correlating structure with intermolecular coupling and dynamics. *Nat. Commun.* **2014**, *5*, 3587. [[CrossRef](#)] [[PubMed](#)]
121. Brehm, M.; Taubner, T.; Hillenbrand, R.; Keilmann, F. Infrared spectroscopic mapping of single nanoparticles and viruses at nanoscale resolution. *Nano Lett.* **2006**, *6*, 1307–1310. [[CrossRef](#)]

122. Meyns, M.; Primpke, S.; Gerdt, G. Library based identification and characterisation of polymers with nano-FTIR and IR-sSNOM imaging. *Anal. Methods* **2019**, *11*, 5195–5202. [[CrossRef](#)]
123. Amenabar, I.; Poly, S.; Goikoetxea, M.; Nuansing, W.; Lasch, P.; Hillenbrand, R. Hyperspectral infrared nanoimaging of organic samples based on Fourier transform infrared nanospectroscopy. *Nat. Commun.* **2017**, *8*, 14402. [[CrossRef](#)] [[PubMed](#)]
124. Bensmann, S.; Gaußmann, F.; Lewin, M.; Wüppen, J.; Nyga, S.; Janzen, C.; Jungbluth, B.; Taubner, T. Near-field imaging and spectroscopy of locally strained GaN using an IR broadband laser. *Opt. Express* **2014**, *22*, 22369–22381. [[CrossRef](#)] [[PubMed](#)]
125. Wu, C.-Y.; Wolf, W.J.; Levartovsky, Y.; Bechtel, H.A.; Martin, M.C.; Toste, F.D.; Gross, E. High-spatial-resolution mapping of catalytic reactions on single particles. *Nat. Cell Biol.* **2017**, *541*, 511–515. [[CrossRef](#)]
126. Zhou, X.-X.; Hao, L.-T.; Wang, H.-Y.-Z.; Li, Y.-J.; Liu, J.-F. Cloud-point extraction combined with thermal degradation for nanoplastic analysis using pyrolysis gas chromatography–mass spectrometry. *Anal. Chem.* **2018**, *91*, 1785–1790. [[CrossRef](#)] [[PubMed](#)]
127. Davranche, M.; Lory, C.; Le Juge, C.; Blanche, F.; Dia, A.; Grassl, B.; El Hadri, H.; Pascal, P.-Y.; Gigault, J. Nanoplastics on the coast exposed to the North Atlantic Gyre: Evidence and traceability. *NanoImpact* **2020**, *20*, 100262. [[CrossRef](#)]
128. Blanche, F.; Davranche, M.; El Hadri, H.; Grassl, B.; Gigault, J. Nanoplastics identification in complex environmental matrices: Strategies for polystyrene and polypropylene. *Environ. Sci. Technol.* **2021**, *55*, 8753–8759. [[CrossRef](#)]
129. Dümichen, E.; Eisentraut, P.; Gerhard, C.; Barthel, A.; Senz, R.; Braun, U. Fast identification of microplastics in complex environmental samples by a thermal degradation method. *Chemosphere* **2017**, *174*, 572–584. [[CrossRef](#)]
130. Dümichen, E.; Barthel, A.-K.; Braun, U.; Bannick, C.G.; Brand, K.; Jekel, M.; Senz, R. Analysis of polyethylene microplastics in environmental samples, using a thermal decomposition method. *Water Res.* **2015**, *85*, 451–457. [[CrossRef](#)]
131. Reichel, J.; Graßmann, J.; Letzel, T.; Drewes, J. Systematic development of a simultaneous determination of plastic particle identity and adsorbed organic compounds by thermodesorption—pyrolysis GC/MS (TD-Pyr-GC/MS). *Molecules* **2020**, *25*, 4985. [[CrossRef](#)]
132. Duemichen, E.; Eisentraut, P.; Celina, M.; Braun, U. Automated thermal extraction-desorption gas chromatography mass spectrometry: A multifunctional tool for comprehensive characterization of polymers and their degradation products. *J. Chromatogr. A* **2019**, *1592*, 133–142. [[CrossRef](#)]
133. Goedecke, C.; Dittmann, D.; Eisentraut, P.; Wiesner, Y.; Schartel, B.; Klack, P.; Braun, U. Evaluation of thermoanalytical methods equipped with evolved gas analysis for the detection of microplastic in environmental samples. *J. Anal. Appl. Pyrolysis* **2020**, *152*, 104961. [[CrossRef](#)]
134. Braun, U.; Eisentraut, P.; Altmann, K.; Kittner, M.; Duemichen, E.; Thaxton, K.; Kleine-Benne, E.; Anumol, T. *Accelerated Determination of Microplastics in Environmental Samples Using Thermal Extraction Desorption-Gas Chromatography/Mass Spectrometry (TED-GC/MS)*; Agilent Technologies Inc.: Santa Clara, CA, USA, 2020.
135. Velimirovic, M.; Tirez, K.; Verstraelen, S.; Frijns, E.; Remy, S.; Koppen, G.; Rotander, A.; Bolea-Fernandez, E.; Vanhaecke, F. Mass spectrometry as a powerful analytical tool for the characterization of indoor airborne microplastics and nanoplastics. *J. Anal. At. Spectrom.* **2021**, *36*, 695–705. [[CrossRef](#)]
136. Yakovenko, N.; de Carvalho, A.R.; ter Halle, A. Emerging use thermo-analytical method coupled with mass spectrometry for the quantification of micro(nano)plastics in environmental samples. *TrAC Trends Anal. Chem.* **2020**, *131*, 115979. [[CrossRef](#)]
137. Mayhew, C.A.; Herbig, J.; Beauchamp, J.D. Proton transfer reaction mass spectrometry. In *Breathborne Biomarkers and the Human Volatilome*; Elsevier: Amsterdam, The Netherlands, 2020; pp. 155–170.
138. Holzinger, R.; Williams, J.; Herrmann, F.; Lelieveld, J.; Donahue, N.M.; Röckmann, T. Aerosol analysis using a Thermal-desorption proton-transfer-reaction mass spectrometer (TD-PTR-MS): A new approach to study processing of organic aerosols. *Atmos. Chem. Phys.* **2010**, *10*, 2257–2267. [[CrossRef](#)]
139. Peacock, M.; Materić, D.; Kothawala, D.N.; Holzinger, R.; Futter, M.N. Understanding dissolved organic matter reactivity and composition in lakes and streams using proton-transfer-reaction mass spectrometry (PTR-MS). *Environ. Sci. Technol. Lett.* **2018**, *5*, 739–744. [[CrossRef](#)]
140. Materić, D.; Ludewig, E.; Xu, K.; Röckmann, T.; Holzinger, R. Brief communication: Analysis of organic matter in surface snow by PTR-MS—implications for dry deposition dynamics in the Alps. *Cryosphere* **2019**, *13*, 297–307. [[CrossRef](#)]
141. Badia, J.; Strömberg, E.; Karlsson, S.; Ribes-Greus, A. The role of crystalline, mobile amorphous and rigid amorphous fractions in the performance of recycled poly (ethylene terephthalate) (PET). *Polym. Degrad. Stab.* **2012**, *97*, 98–107. [[CrossRef](#)]
142. Wu, P.; Tang, Y.; Cao, G.; Li, J.; Wang, S.; Chang, X.; Dang, M.; Jin, H.; Zheng, C.; Cai, Z. Determination of environmental micro(nano)plastics by matrix-assisted laser desorption/ionization—time-of-flight mass spectrometry. *Anal. Chem.* **2020**, *92*, 14346–14356. [[CrossRef](#)]
143. Yang, C.; Lee, H.K.; Zhang, Y.; Jiang, L.-L.; Chen, Z.-F.; Chung, A.C.K.; Cai, Z. In situ detection and imaging of PFOS in mouse kidney by matrix-assisted laser desorption/ionization imaging mass spectrometry. *Anal. Chem.* **2019**, *91*, 8783–8788. [[CrossRef](#)] [[PubMed](#)]
144. Lin, Y.; Huang, X.; Liu, Q.; Lin, Z.; Jiang, G. Thermal fragmentation enhanced identification and quantification of polystyrene micro/nanoplastics in complex media. *Talanta* **2020**, *208*, 120478. [[CrossRef](#)] [[PubMed](#)]